Equilibrium Particulate Exposure

Lorenzo Aldeco
Banco de México *
Lint Barrage
ETH Zurich †
Matthew A. Turner
Brown University ‡§

30 March 2026

Abstract: How should we measure air quality benefits of environmental taxes? Taking a general equilibrium perspective, this paper argues that reductions in particulate *emissions* or *concentrations* are neither necessary nor sufficient to ensure reductions in population pollution *exposure*. First, using global spatially disaggregated panel data on ambient particulates and population, we show that countries' changes in particulate *exposure* can be substantially larger or smaller than their changes in concentrations. Second, we develop a macroeconomic integrated assessment model of particulate exposure for 30 countries (representing 60% of world population) to evaluate the relevance of this point for policy. We find that both uncompensated oil taxes and agricultural burning levies may unintentionally *increase* exposure despite decreasing targeted activity emissions by shifting labor to dirtier sectors or locations. Third, however, we also find that income support can counteract these effects and greatly increase the environmental effectiveness of fossil energy taxes. Overall, our results demonstrate the importance of considering *exposure* in environmental policy evaluations.

Keywords: Particulates, Air Pollution, Integrated Assessment, Tax Policy, General Equilibrium, Second best environmental policy, Revenue Recycling

JEL: E62, H23, Q53, Q58

*Banco de México. Av 5 de Mayo 18, Col. Centro, 06000, Mexico City, Mexico. email: lorenzo.aldeco@banxico.org.mx.

†Chair of Energy and Climate Economics, Department of Management, Technology, and Economics, ETH Zurich, Zurichbergstrasse 18, 8092 Zurich, Switzerland. email: lbarrage@ethz.ch. Also affiliated with CEPR and CESifo.

‡Department of Economics, Box B, Brown University, Providence, RI 02912. email: matthew_turner@brown.edu. Also affiliated with PERC, IGC, NBER, and PSTC.

§The authors gratefully acknowledge financial support from IGC grants 1-VRU-VXX-X-VXXXX-89451 and 1-VRE-VNEC-VXXXX-89467 and from the PSTC at Brown University. Turner gratefully acknowledges the hospitality and support of PERC during part of the time this research was conducted.

1. Introduction

According to the Global Burden of Disease Project (GBD, 2024), ambient airborne particulates kill about 4.7m people per year. The value of statistical life in a country with global average GDP per capita is plausibly around 2.8m (USD2010).[1] The product of these two numbers is 13 trillion dollars. This is more than 10% of global annual GDP. This estimate can be too large by orders of magnitude and still establish that managing particulate exposure is an important problem.

Governments typically respond to this problem with two main approaches. Regulatory tools - such as air quality or technology standards - are well-established in advanced economies (e.g., U.S. Clean Air Act) but face enforcement challenges in emerging markets (e.g., Duflo, Greenstone, Pande, and Ryan (2013)). Fiscal tools such as fossil fuel taxes are also widely used.[2] Indeed, the International Monetary Fund (Parry, Heine, Lis, and Li (2014); Black, Celniak, Garcia-Huitrón, Parry, Schulz Antipa, and Vernon-Lin (2025)) and World Bank (WB (2021)). frequently recommend increasing such taxes in part because of expected health benefits from air quality improvements. These estimated benefits, however, are generally based on frameworks assuming limited population adjustments to pollution or policy.

This paper revisits both the measurement and modeling of environmental tax effects on particulate exposure from a general equilibrium perspective. First, we combine spatially disaggregated global panel data describing aerosol optical depth, a remotely-sensed measure of particulate concentration, with a global panel of gridded population data. This combination allows us to measure particulate *exposure*, the coincidence of people and pollution. This allows us to establish the importance of spatial equilibrium adjustments for particulate exposure: Countries' observed changes in particulate *exposure* can be substantially larger (e.g., +50% in Poland) or smaller (e.g., -80% in Indonesia) than their contemporaneous changes in particulate *concentrations*. Intuitively, the locations of people and particulates concentration both change in response emissions regulation. Analyses that do not account for such adjustments may thus substantially over- or under-estimate environmental taxes' benefits.

[1]We take the US EPA value of statistical life (VSL) of \$7.4m in USD2006 converted to around \$8m in USD 2010, an income elasticity of VSL of 0.6 from Viscusi and Aldy (2003), global and US income per capita of about 11,000 and 63,000 in USD2010 (in 2022), respectively, which yield $(8 \times 10^6)(\frac{11{,}000}{63{,}000})^{0.6} \approx 2.8 \times 10^6$.

[2]Among countries with available tax data for 2022 from IEA (2024), the majority tax petroleum products (70% or 41 out of 59), and many tax coal (50% or 19 out of 38). These figures exclude indirect VAT and carbon levies. OECD (2019) similarly finds fuel taxes in 44 major economies. At the same time, IEA (2023) identifies 22 countries subsidizing oil (2 subsidizing coal) directly. These countries have been encouraged to reduce fuel subsidies in part due to expected air pollution health benefits.

Second, we develop a new macroeconomic integrated assessment model of equilibrium exposure and quantify it for 30 countries that account for about 60% of the world's population. Both the structural design and quantification of the model are informed by a set of stylized facts we document from our exposure data. One of these facts is the critical importance of country-specific factors in determining particulate exposure. Informed by this finding, we quantify the model using detailed country-specific data describing baseline energy use by fuel and sector (e.g., the extent to which the agricultural sector relies on oil in Bangladesh vs. Poland) from the International Energy Agency, and on country-specific particulate emissions coefficients both for fuels (e.g., coal emissions coefficients in China vs. Korea) and activities (e.g., agricultural residue burning per unit of agricultural output in Indonesia vs. Brazil) from IIASA. The model features multiple sectors, multiple energy sources, multiple sources of particulate emissions, and endogenizes spatial adjustments in both production and population.

Third, we use the model to evaluate the counterfactual impacts of environmental taxes on particulate exposure and welfare. The results indicate that partial equilibrium estimates of policy impacts on particulate *emissions* can be quantitatively and qualitatively incorrect as proxies for changes in exposure. For example, uncompensated petroleum taxes are projected to *increase* aggregate particulate exposure in most model countries. Intuitively, this occurs because both the decrease in real incomes and the disproportionate effect on the oil reliant agricultural sector push rural workers into more polluted urban areas (and potentially more polluting sectors). For levies on agricultural residue burning - a major source of particulate pollution in many countries - the model predicts a substantial decrease in *emissions* which often does not translate into reductions in *exposure*, again because of the reallocation of agricultural workers. Coal taxes, in contrast, appear broadly effective at reducing particulate exposure. Quantitatively, however, equilibrium adjustments remain important. For example, in South Africa, the model's predicted partial equilibrium emissions reduction benefits from uncompensated coal levies are about double the projected reduction in equilibrium exposure. Importantly, however, these unintended consequences can often be mitigated by accompanying levies with income support (lump-sum rebates). Such rebates can mitigate the pressure for rural workers to take higher paying jobs in more polluted locations, thus increasing the effectiveness of environmental levies. While the *economic* benefits of targeted environmental tax revenue use are well-established, to the best of our knowledge, the finding that rebates can determine whether levies improve environmental outcomes is new.

This work relates to several strands of literature. First, we build on the long and influential tradition of integrated environment-economy models (IAMs), most directly growing efforts to analyze environmental processes in general equilibrium. Most of this work considers climate change (Dietz, 2025). While this literature has produced fundamental and relevant insights for our analysis (as discussed below), it is important to note that the economics of particulate pollution differs fundamentally from climate change. Climate change is a global stock pollutant problem largely driven by fossil energy consumption. Consequently, the spatial distribution of emissions sources is irrelevant, dynamics are first order, and a one-sector model accounts for policy impacts on energy input choices (e.g., Golosov, Hassler, Krusell, and Tsyvinski (2014)) can cover the main emissions sources. Particulates, in contrast, are a flow pollutant for which country- and region-specific emissions are first order (as we show) and which stem from a wide range of sources whose relative importance varies by country.

To the best of our knowledge, only a handful of papers model particulates in general equilibrium (GE). Some studies have considered particulates in single-region, multi-sector GE models of the United States. While these studies have demonstrated both the potential for meaningful emissions changes from fossil energy taxes (Goulder and Hafstead (2018)) and that partial equilibrium may over- or under-estimate the welfare effects of these taxes (Carbone and Smith (2008)), single-region models cannot distinguish concentrations from exposure. Hollingsworth, Jaworski, Kitchens, and Rudik (2024) develop an economic geography IAM specific to the United States to analyze air quality regulations in spatial equilibrium. Their results show large welfare gains that would have been substantially underestimated by an analysis ignoring the movement of pollution, workers, and activity across space. Khanna, Liang, Mobarak, and Song (2024) develop a quantitative model to estimate the aggregate productivity consequences of exogenous changes in particulate pollution in China. Their results also demonstrate the importance of equilibrium adjustments, the migration response to particulate concentration in particular. Importantly, however, neither of these papers is set up to study fossil energy taxes as neither models energy inputs to production.[3] Similarly, as neither of these studies models the agricultural sector, they also cannot speak to burning levies nor the relative impacts of, e.g., oil taxes on this sector. While our framework offers reduced detail in other dimensions, such as coarser geography, our analysis thus offers a new perspective on highly policy-relevant questions. We also estimate policies' effects across 30 countries.

Our focus on particulates and on multiple sectors, emissions sources, and energy in-

[3]Hollingsworth et al. (2024) model particulate pollution directly as an input to production whose shadow price is determined by regulations. Khanna et al. (2024) model particulates in reduced-form as function of local employment.

puts also distinguishes our model from the growing frontier in spatial climate economics (e.g., Cruz and Rossi-Hansberg (2024); Burzyński, Deuster, Docquier, and De Melo (2022)). Though richer in several dimensions, such as spatial resolution, given the nature of climate change this literature often does not distinguish fossil energy inputs (e.g., coal vs. gas) or features only one or two sectors. Some of our results nonetheless relate, such as on the potential benefits of local revenue rebates (Conte, Desmet, and Rossi-Hansberg, 2025), though the mechanisms are fundamentally different.

Second, our work relates to broader interdisciplinary modeling efforts to quantify the air pollution benefits of fossil taxes and related policies (Karlsson, Alfredsson, and Westling (2020)). Though often highly detailed in their representation of technologies and emissions sources, these models generally do not consider the types of equilibrium responses to pollution and policy that are the focus of our analysis. For example, the seminal AP3 model tracks emissions, concentrations, and damages for several pollutants including $PM_{2.5}$ across U.S. counties (see, e.g., Muller and Mendelsohn (2007, 2009), Holland, Mansur, Muller, and Yates (2016), Tschofen, Azevedo, and Muller (2019) and also the InMAP model by Tessum and Marshall (2017)). Though rich and spatially detailed, these models take the locations of people and firms as given. Similarly, the International Institute for Applied Systems Analysis' GAINS model ("Greenhouse gas - Air pollution Interactions and Synergies") features an extremely detailed representation of emissions sources, accounting for details such as the distributions of boiler types and livestock species across countries. However, GAINS is not an equilibrium-based model and does not consider the behavioral responses that are our focus. We nonetheless build on GAINS in our model quantification, as other scholars have done (e.g., Parry et al. (2014)). Finally, even analyses in this literature that are based on general equilibrium models typically have coarse regional resolution (e.g., "Europe" as one region) and treat population as fixed, again implicitly equating changes in concentrations and exposure (e.g., Reis, Drouet, and Tavoni (2022)).

Third, our analysis relates to empirical literatures on particulate pollution. One strand of literature has causally demonstrated large adverse health effects from particulate exposure (e.g., Chay and Greenstone (2005), Arceo, Hanna, and Oliva (2016), Chen, Ebenstein, Greenstone, and Li (2013), Knittel, Miller, and Sanders (2016), Deryugina, Heutel, Miller, Molitor, and Reif (2019)), motivating our analysis. Another strand studies particulate policy. Perhaps the most widely studied policy in this context is the U.S. Clean Air Act (CAA), a collection of regulations that impose restrictions on emissions in regions of the US that fail to attain mandated standards for air quality, including levels of particulates (see Currie and Walker (2019) and Aldy, Auffhammer, Cropper, Fraas, and Morgenstern (2022)). Though effective at reducing particulate concentrations (Chay and Greenstone (2005)), the CAA also led to a substantial reallocation of employment and industry across space (Greenstone (2002); Walker (2013))[4]. Recent empirical work also establishes significant migration responses to air quality in China (Chen, Oliva, and Zhang, 2022, Khanna et al., 2024).

In short, the existence of the sorts of general equilibrium effects with which we are concerned is empirically established for a specific US regulation and select emerging markets. Regulation of particulates can lead to the migration of firms and workers across sectors and regions.

With this said, it is hard to guess from the available results what, for example, the equilibrium effects of agricultural burning restrictions in Pakistan or coal taxes in Poland would be. Empirical evidence causally linking such taxes to particulate exposure is surprisingly scarce.[5] This is the type of question we thus hope to address with our analysis, thereby also bringing a macro perspective to the literature on developing country particulates policy (Greenstone, Pande, Sudarshan, and Ryan, 2024, Jack, Jayachandran, Kala, and Pande, 2024, Davis, 2008, Duflo et al., 2013, Oliva, 2015).

The remainder of this paper proceeds as follows. Section 2 empirically motivates our approach and analysis. Section 3 describes the data used in our empirical analysis. Section 4 summarizes the descriptive results that inform our model design. The model and its quantification are described in Sections 5 and 6, respectively. Section 7 describes the counterfactual results, with sensitivity analysis in Section 8. Section 9 concludes.

2. The geography of particulate exposure

Particulates arise as a consequence of emissions. Emissions, from whatever source, are measured in units of mass (megatonnes (MT) or kilotonnes (KT)).[6] Point source regulation is generally concerned with regulating the mass of emissions. Once in the air, particulates disperse. This leads to a certain mass per volume of air. This is the concentration of particulates. The units of concentration are mass per unit volume, and this is what

[4]Greenstone (2002) finds that regulation decreased employment by about 600,000 in non-attainment regions between 1972 and 1987, on the order of 1% of US employment during this time.

[5]For concentrations evidence is also limited and arguably mixed. Kheiravar and Lawell (2020) fail to detect declines in particulate concentrations from fuel subsidy reductions in Iran (except when accompanied by gasoline quotas). In contrast, Basaglia, Behr, and Drupp (2023) find substantial particulate reductions from fuel taxes in Germany. Hernandez-Cortes and Meng (2023) find particulate reductions due to California's carbon market, as do Basaglia, Grunau, and Drupp (2024) for the EU ETS. In contrast, Venkataramani and Fried (2011) associate higher oil prices in Guatemala with increased biomass use and worsened child respiratory health.

[6]We focus on *primary* particulate emissions throughout.

Figure 1: Population, particulates and exposure

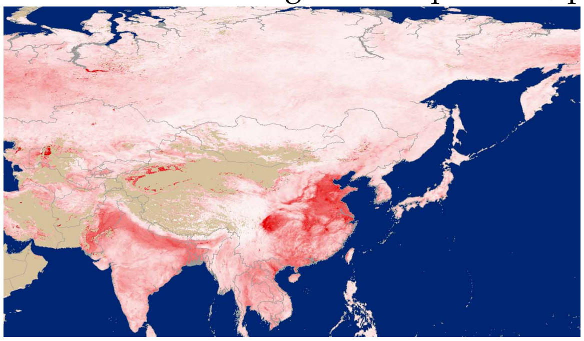

(a) AOD, Terra 2010

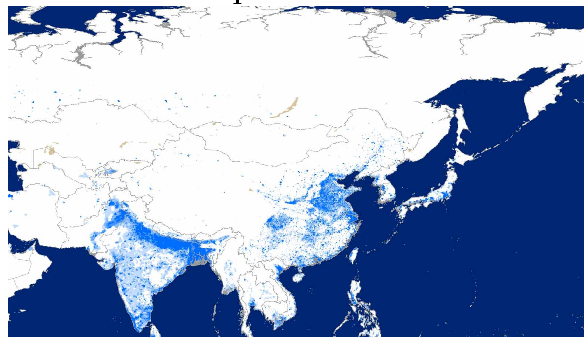

(b) Population, GPW 2010

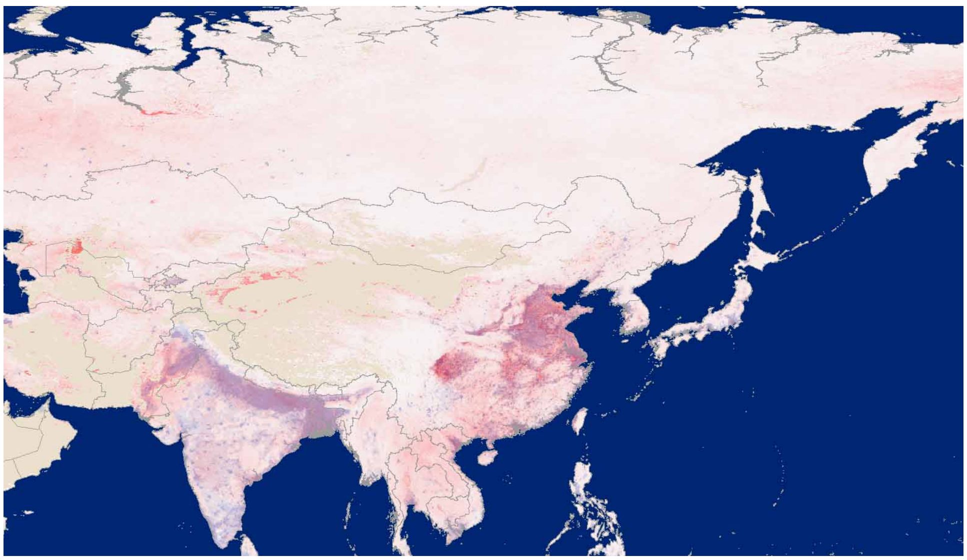

(c) Exposure, 2010

is measured by most pollution monitors. We will generally measure concentration in kg/km^3 (or equivalently, μg/m^3). We sometimes also measure concentration in terms of "aerosol optical depth" (AOD). This is the measure of concentration reported by our remotely sensed pollution data (discussed below.) We exclusively consider outdoor ambient concentration. Indoor air pollution is also of interest, but data limitations preclude its consideration. We are primarily concerned with exposure. For our purposes, this will be the person weighted mean of concentration, and its units are AOD points per person. This definition is tractable and transparent, but implicitly assumes that individual exposure is linear in concentration.[7]

These definitions allow a description of concentration and exposure. Figure 1 presents three maps showing China, India and Russia, among other countries (see Online Appendix for global versions). Panel (a) shows the distribution of AOD in 2010. Darker

[7]Damages from exposure are convex in our model.

red indicates higher mean annual particulate levels. Tan indicates missing data. Unsurprisingly, China is highly polluted, particularly in the central region and the Northeast. India is also highly polluted, particularly in Ganges river valley, although we also see high levels of particulates throughout the subcontinent. Russia is generally less polluted, and its particulates occur mainly in the West.

Panel (b) shows population density, also in 2010. China is densely populated except for provinces on its Western frontier. Population is particularly dense in the central region around Chongqing and in the Northeast. Even away from these areas, population appears to be highly concentrated into cities. Population density in India is also high, especially along the Ganges, although even away from this region, population density is almost uniformly high. Russia, in contrast, appears almost unpopulated, although small cities are visible, mostly in the Southern part of the country.

Panel (c) superimposes panel (a) on panel (b). The interpretation of colors is then as follows: White indicates areas with low population and low particulates. Pink and red indicate areas with high particulates and low population. Blue indicates regions with high population density and low particulates. Purple indicates regions with high particulates and high population density. That is, purple indicates regions where many people are exposed to high concentrations of particulates.

Panel (c) illustrates two features of our data that recur throughout our analysis. First, exposure is substantially determined by country of residence. Second, the geography of particulates matters. In Russia, particulates tend to occur away from population centers. In India and China concentration and population coincide, although India is more "blue" while China is more "pink". In India, highly populated and polluted places are surrounded by places that are highly populated, but not as polluted. China is the opposite. Highly populated and polluted places are surrounded by places that are highly polluted, but not as densely populated. Moving out of the densest cities looks like a better response to particulates in India than in China.

Table 1 reinforces and refines these observations based on data for a selection of countries accounting for almost 50% of the world's population. The first column presents an area weighted mean of AOD - *concentrations* - in 2010 for each country. The second column presents our *exposure* measure, population weighted mean AOD.

In line with discussion above, Table 1 shows that, while China and India had similar average particulate *concentrations* in 2010, *exposure* was substantially higher in China. Similarly, Brazil, Russia, and the United States also share similar average air quality, exposure is 60-70% larger in Russia and the US than in Brazil. We also see that, while

Table 1: Levels and changes in concentration and exposure for several countries

	AOD 2000	Mean exposure 2000	$\%\Delta$ AOD 2000-10	$\%\Delta$ Mean exposure 2000-10	$\frac{\%\Delta \text{AOD}}{\%\Delta \text{Exposure}}$
China	0.31	0.52	13.60	23.02	0.59
India	0.28	0.35	31.02	30.00	1.03
Brazil	0.13	0.10	65.95	32.53	2.03
Russia	0.12	0.16	52.26	74.18	0.70
US	0.14	0.17	-20.99	-14.67	1.43
Indonesia	0.20	0.26	-16.15	-3.45	4.68
Poland	0.20	0.21	-5.21	-7.92	0.66
Australia	0.07	0.08	-13.87	4.38	-3.17

Note: *This table shows descriptive statistics on levels and growth rates of particulate measures and exposure, for selected countries. AOD data is from NASA's MODIS, measured by the Terra satellite (Levy, Hsu, et al., 2015a). Exposure is the population-weighted AOD average across pixels. Population data is from Gridded Population of the World (CIESIN, 2016).*

exposure typically exceeds concentration, people are more likely to live in polluted areas, this is not the case for Brazil. In short, the first two columns of table 1 confirm what we see in figure 1. Countries matter, as does the within country geography of population and concentration.

The next two columns report percentage changes in AOD and exposure between 2000 and 2010. Indonesia saw AOD fall by about 16%, but exposure by only 3.45%. Thus, Indonesia accomplished a dramatic reduction in concentration, but this reduction did not occur in places where people lived (or people migrated to more polluted places). Conversely, over the same time period, Poland achieved exposure reductions that were about 50% larger than their reductions in concentration. As the last column of Table 1 shows, countries' changes in particulate exposure are often dramatically larger or smaller than their changes in air quality. Australia provides an example where changes in average concentrations (air quality) are even of the opposite *sign* as for exposure: While air quality improved on average, exposure increased as people and pollution were moved closer together.

In sum, Table 1 and figure 1 showcase the importance of considering and endogenizing *exposure* in air quality policy assessments. The results also suggest the importance of country level factors.

Table 2 complements these conclusions by describing the contributions of various economic activities to concentration by country. For reference, the first column reports mean annual concentration of particulates for 2010 in kg/km^3. The subsequent columns express the particulate emissions from a particular class of activities as a concentration. This value is the ratio of two quantities. The numerator is the mass of particulate

Table 2: Country level select emissions in concentration units for 2010

	Ambient	Coal	Oil	Ag. burning	Flow out	Flow in	Service process	Ind. process
Indonesia	17	1	19	205	321	354	0	4
Brazil	22	2	28	52	138	161	6	26
US	11	49	53	38	128	129	33	24
India	36	1481	286	379	249	379	17	436
China	36	3256	208	318	311	324	17	1301
Poland	19	3875	107	12	195	214	42	59
Six country average	23	1444	117	167	224	260	19	308
Pixel average (sample size= 26,169,345 pixels)	23	958	104	155	200	227	17	357

Note: *This table shows ambient concentration and emissions expressed in concentration units for selected countries and emission sources. Coal, oil, industry and service emissions are from IEA. Agricultural burning data is from IIASA. Flow in and out are own calculations using AOD measurements and wind data from Wentz et al. (2015).*

emissions from a particular source in 2010.[8] The denominator is the mixing volume of each country, the area of the country times the mixing height. We postpone a discussion of data sources. Thus, the total particulates from coal combustion in China in 2010 contributed 3256 kg/km^3 of particulates to China's entire mixing volume. The top panel of table 2 reports country level calculations. The bottom panel presents two aggregate calculations. The country average is calculated by first performing our calculation for each country and then averaging, giving each country equal weight. The pixel average is an average over countries, weighting each country by its mixing volume.

Table 2 suggests three conclusions. First, the flow of particulates into the atmosphere in a year is large compared to the average ambient concentration. On average emissions have a short residence time in the atmosphere, or equivalently, the deposition rate is high relative to the emission rate. In section 5 we develop a model of the way that particulates enters and exits the atmosphere. The high ratio of particulate emissions to average concentration motivates our decision to model this process in steady state.

Second, the bottom panel of table 2 suggests an approximate ranking of the importance of different activities for particulates concentration. *On average*, coal is by far the most important source of particulate emissions. Oil and agricultural burning are both important, but are an order of magnitude less important than coal. Flows of particulates into countries' mixing volumes from the rest of the world are about double the mass of emissions from oil or agricultural burning (on average), but are almost perfectly offset by outflows. Unsurprisingly, the service sector contributes little to emissions. Process emissions from heavy industry are the most important contributor after coal.

[8] The listed sources are not exhaustive as, e.g., natural processes such as sand storms also contribute to particulates. These are considered in the quantitative model.

Third, the top panel of table 2 presents country level statistics which demonstrate again the first order importance of country heterogeneity. In figures 1 and OA1, and in table 1 we see that particulate concentration and its distribution across populous and unpopulous places differs across countries. In table 2 we see that the portfolio of polluting economic activity also differs across countries. For example, agricultural burning is a vastly larger emissions source than coal in countries such as Brazil or Indonesia. These patterns motivate and highlight the value of both our multi-country and multi-sectoral approach.

3. Data

The objects of this project are to (1) describe patterns of exposure and to (2) investigate the relationship between equilibrium levels of exposure and various covariates in order to (3) develop and quantify a particulates integrated assessment model.

Steps (1) and (2) require three types of data. The first is gridded panel data of concentration and population. The second are measures of the physical environment that affect the deposition, dispersion or natural sources of particulates, e.g., climate, wind and land cover. The third is descriptions of polluting activities such as fuel use. Here we briefly describe each class of data, relegating technical details to the Appendix. We also postpone descriptions of additional data required for Step (3) to Section 5.

A *AOD and population*

We rely on a remotely-sensed measure of particulate concentration, aerosol optical depth, provided by the NASA Terra satellite using the Moderate Resolution Imaging Spectroradiometer (MODIS) (Levy, Hsu, and al., 2015). MODIS records the intensity of the light reflected into space from the surface of the Earth. Comparing this measured intensity with a reference value allows an estimate of the share of light that is dispersed in the air column. More precisely,

$$\text{AOD} = -\ln\left(\frac{\text{light arriving at ground}}{\text{light arriving at top of atmosphere}}\right).$$

That is, AOD is a positive, monotone transformation of the fraction of light arriving at the top of the atmosphere that reaches the ground (Jacob, 1999a). Following the literature, we rescale AOD from $0 - 5000$ to $0 - 5$.

The spatial resolution of the MODIS AOD data is about 3km square and they are available about daily. To ease computation, we reprocess all of our gridded data to a standard grid with a resolution of 0.0833 arc minutes, about 10 kilometers at the equator.

This results in a grid of pixels 4320×1740, with a North-South range from 85 degrees North to 60 degrees South. After reprocessing each daily image into this grid, we average over days within each year. Figure OA1 (a) maps these data for the world in 2010.

Table 3 provides descriptive statistics for our AOD data in 2000 and 2010. The left two columns describe the 233 countries covered by our gridded population and AOD data, while the right two columns describe the 30 countries for which we calibrate our IAM, our main sample. The 233 countries described in the left two columns contain about 6.34b people in 2010. In 2000, world average AOD was 0.17 and this increased to 0.20 by 2010. Exposure, person weighted mean AOD, was higher and increased faster, from 0.33 in 2000 to 0.38 by 2010. Thus, people tend to concentrate in more polluted places.

Turning to the right two columns, in 2000, average AOD in our main sample was 0.15 and this increased to 0.19 by 2010. Exposure in 2000 was 0.36 increasing to 0.44 by 2010. This sample contains about 0.91m pixels and 4.10b people. Thus, our main sample describes about 65% of the population reported in the larger sample and covers about 60% of the area. Concentration in the main sample is marginally lower than in the universe, and exposure is somewhat higher. This is consistent with the main sample of countries being somewhat larger, more developed and more urban than the full sample.

We are interested in the concentration of particulates in the air, mass per unit volume. We convert AOD to concentrations with the conversion factor $\rho = 100\mu\text{g/m}^3$ PM10 suggested by Gendron-Carrier, Gonzalez-Navarro, Polloni, and Turner (2022). Thus, an AOD measure of 1 in one of our nominally 10km^2 pixels maps to an annual average concentration of $100\mu\text{g/m}^3$ PM10.

Particulates cause health problems when people come into contact with them, while MODIS measures AOD throughout the whole air column. Ideally, we would measure particulate concentration at ground level (see, e.g., Hidy et al. 2009). While several studies have developed modeling tools and data products designed to yield more precise estimates of ground level particulates (e.g., Brauer et al. 2015; Van Donkelaar, Martin, Brauer, Hsu, Kahn, Levy, Lyapustin, Sayer, and Winker 2016), these typically combine MODIS data with inputs that are correlated with population density. For our purposes, this leads to difficulties in the interpretation of correlations that do not arise with the raw MODIS AOD data, which we therefore prefer. While this choice may leave noise in our approximation of particulate concentrations, we note that (i) the qualitative results of our data analysis, such as the importance of distinguishing concentrations from exposure, also arises in these alternative data products, and (ii) our central contribution is to highlight novel *economic* equilibrium adjustments to fossil energy taxes.

We measure population using version 4 of Gridded Population of the World (CIESIN,

Table 3: Descriptive statistics

	Whole World (233 Countries)		Main Sample (30 Countries)	
	2000	2010	2000	2010
AOD	0.17	0.20	0.15	0.19
Exposure	0.33	0.38	0.36	0.44
Pop (000,000)	5,627	6,341	3,704	4,102
Area (00km^2)	954,833	954,833	529,026	529,026
Pixels	1,512,023	1,512,023	910,150	910,150

Note: *Description of particulate concentration and exposure for the whole world (top) and for 30 country sample on which most of our analysis is based (bottom). AOD data is from NASA's MODIS, measured by the Terra satellite (Levy et al., 2015). Exposure is the population-weighted AOD average across pixels. Population data is from Gridded Population of the World (CIESIN, 2016). The 30 countries described by the bottom panel are; Australia, Bangladesh, Belarus, Bosnia and Herzegovina, Brazil, Bulgaria, China, Croatia, Czech Republic, Estonia, Greece, Hungary, India, Indonesia, Lithuania, Malaysia, Pakistan, Poland, Portugal, Republic of Korea, Romania, Russian Federation, Serbia, Slovakia, South Africa, Thailand, Turkey, Ukraine, UK, and the US.*

2016), for 2000, 2005, 2010, and 2015. These data are based exclusively on administrative data describing population. They are constructed by assigning population to about 1 km square pixels (0.0083 degrees) and interpolating to provide pixel based population estimates in modulo five years. We reprocess these data by consolidating pixels into 10×10 groups. The resulting 0.083 degree grid is the basis for our gridded data. Figure OA1(b) presents a map of our population data for 2010.

B *Climate*

Climate is important for our analysis for three reasons. First, relative to ground based instruments, MODIS is less able to distinguish water vapor (particles of water) from the dust and soot that is our main concern. Consequently, controlling for local measures of water vapor may be important in regression analysis. Second, MODIS only operates on cloud-free days, and so climate has a direct impact on the selection of days and pixels where we measure AOD. Third, climate may affect concentration directly because rainfall contributes to wet deposition of particulates.

We rely on data from CRU (Jones and Harris (2013)) for monthly gridded measures of climate. These data are available with a spatial resolution of 0.5 degrees. We reprocess them to our finer grid and average over months to create annual measures. In particular, we calculate annual means of, days of cloud cover, mean daily precipitation, mean daily vapor pressure, mean daily temperature, and days with frost.

C *Emissions*

We measure cross-border particulate flows, fossil fuel use and economic activity at the country level. At the pixel level, we measure three other sources of particulates; urbanization, land cover and fires.

Fossil and organic fuels: Combustion is a major source of particulates. We focus on two kinds of economically important combustion, modern energy and biomass burning.

We observe consumption of three main fuel groups, by country, year, and economic sector. The groups are, as defined by the International Energy Agency (IEA): coal, peat, and oil shale (from here on, coal); crude oil, oil products, natural gas liquids, and refinery feedstocks (from here on, oil); and natural gas along with other clean energy sources, including solar, nuclear, geothermal, and wind (from here on, gas/green). To facilitate aggregation across fuels, all energy consumption is measured in million tonnes of oil equivalent (Mtoe). Figure OA2 (a) illustrates the intensity of coal consumption per unit area in 2010, with darker gray indicating more intensive coal use, lighter gray indicating less coal use, and tan indicating missing data.

We observe organic fuel (also called biomass) consumption for about 60 countries (the actual number varies slightly by fuel and year), as reported by the International Institute of Applied Systems Analysis (IIASA). Biomass consumption is measured in petajoules (PJ) and includes household use of organic fuels like wood, dung, and agricultural byproducts burned for energy generation. Agricultural waste burned for clearing and other non-energy purposes is tracked separately. Figure OA2 (b) illustrates the intensity of organic fuel use in per unit area in 2010, with darker green indicating more intensive use, lighter green indicating less use, and tan indicating missing data.

GDP sector shares and GDP: Both the level and composition of economic activity are important potential determinants of particulate emissions. To measure economic activity by sector, we use country-year level data on the GDP shares of agriculture, industry, and services from the World Bank (World Bank Development Indicators), and data on non-combustion particulate emissions from industry, services, and agriculture from IIASA.

Urban vs rural: Inspection of figure 1 suggests that urban areas are more polluted than rural areas. To measure urban status, we rely on two sources of information. The first is our gridded population data. The second is World Bank (2018), which reports the urban share of each country's population. Using both data sources, for each country, we assign the smallest possible number of pixels to the urban class, subject to reaching the urban population share reported in World Bank (2018). Figure OA2 (c) shows the resulting partition of the world into rural and urban. Our model describes small open economies consisting of rural and urban regions. Our calibration of this model relies on the geography illustrated in figure OA2 (c).

Land cover: Some of our regressions investigate the relationship between land cover and particulates. We rely on MODIS land cover and fire data, (Channan, Collins, and Emanuel (2014) and Giglio and Justice (2015)). The land cover data are annual, gridded data with about 5 km^2 resolution. Each pixel reports one of several land cover classifications, among them, crops and barren. We reprocess these data into our standard grid.[9] MODIS fire data are more complicated. MODIS reports measures of fires at approximately two week intervals for $250m^2$ pixels. To aggregate to our larger pixels and longer periods, we calculate the share of $250m^2$ pixel days of fire that occur in each of our larger and less frequently observed pixels. This is our MODIS fire index.

Cross-border flows: Cross-border flows are sometimes important sources or sinks for particulates. To measure such flows at the country-year level, we must measure pixel level mean annual wind. We rely on Wentz et al., (2015) to measure mean monthly wind speed for a 0.25 degree grid. We aggregate to years and reprocess to match our somewhat finer analysis grid. We are left with two grids describing wind speed. One gives mean wind velocity North to South, and the other East to West. Together with our AOD data, this allows us to calculate the aggregate flow of particulates across any border in our data (kt/year). The details of this calculation are in the appendix.

Using our definition of urban and rural areas, we calculate all cross-border flows at the level of the country-region. Figure OA2 (d) illustrates these flows for 2010. We represent cross-border flows, not by their total mass, but by their capacity to contribute to concentration. That is, we divide by the volume air in which they disperse, the country-region's area times its mixing height. Absent systematic evidence about cross-country differences in mean annual mixing height we fix this quantity for all countries based on detailed estimates from across the United States (see Appendix).

In figure OA2 (d), bright red to white country-regions are net exporters of airborne particulates, light to dark gray country-regions are net importers. Most countries, particularly those with long seacoasts, are net exporters. Central Africa is known for both

[9]The MODIS land cover data also report an "urban" land use code. We experimented with using this code to indicate urban areas. We found that it was less related to population density than our current method. We also investigated changes in the MODIS urban code to track construction, a likely source of particulates. We concluded that the data are too noisy to be informative about new building.

Table 4: Explanatory power of country and year indicators

	(1)	(2)	(3)	(4)	(5)	(6)	(7)
Country FE	Y	.	.	.	Y	.	.
Year FE	.	Y	.	.	.	Y	.
Country $\times$ Year FE	.	.	Y	.	.	.	Y
Climate	.	.	.	Y	Y	Y	Y
30 countries:							
N	3640600	3640600	3640600	3636452	3636452	3636452	3636452
R^2(Area weighted)	0.304	0.014	0.348	0.122	0.420	0.133	0.459
R^2(Population weighted)	0.418	0.020	0.463	0.129	0.524	0.140	0.559

dust storms and agricultural burning, and a handful of these countries are importers. China's southern neighbors are net importers, as are Brazil's southern neighbors. Looking closely at the figure suggests that many European cities export particulates to the surrounding regions.

4. Descriptive and reduced form results

We now investigate variation in exposure and its determinants, with the goal of informing the design of our model. We begin by investigating the importance of country and year level variation in our four year panel of pixels.

Table 4 Column 1 presents the results of four regressions of pixel level AOD on country fixed effects in our main sample of 30 countries. Moving down the column, we first report the number of pixel-years. In the next row, we report the R^2 of this regression, 0.30. That is, with only country indicators we explain 30% of total variation in *pixel* level AOD over 2000, 2005, 2010 and 2015. At first glance, this seems surprising. Very small particles aside, particulates fall out of the air in days to weeks. There is also a literature reporting the rate at which particulate concentrations decay as a function of *meters* from a source, e.g., Cho et al., (2009). Given this prior evidence for the importance of small scale, high frequency variation, the fact that country level variation has so much ability to predict concentration is unexpected. However, recalling figure 1(a), it is less surprising. There are obvious differences in mean annual concentrations across Russia, India and China. Our fixed effect regression establishes the generality of this observation.

The next row of column 1 reports the R^2 of the same regression where pixels are weighted by their population rather than their area, this is effectively regressing exposure rather than concentrations on country fixed effects. We explain 42% of the variation in pixel level exposure in this regression. Knowing only country of residence, we reduce mean square prediction error for individual exposure almost in half. Column 2 parallels column 1, but estimates the effect of year indicators for the four panel years. These have little ability to predict either concentration or exposure. Column 3 includes indicator variables for each country-year pair. These regressions have marginally more predictive power than country variables alone.

In all, columns 1-3 suggest that country level fixed characteristics are important for determining exposure. We would like to establish that this does not simply reflect country specific climate. Column 4 of table 4 reports a regression, like those in columns 1-3, but where the control variables are our four pixel-year level climate variables. We see that the R^2s in these regressions are 0.12 and 0.13, depending on specification. Columns 5-7 of table 4 replicate columns 1-3, but add climate controls. These regressions have higher R^2s than their counterparts without climate controls. They also have higher R^2s than the climate only specification in column 4. Thus, we reach three conclusions. First, climate is important, but country level factors are important independent of climate. Second, country level indicators explain more variation in concentration and exposure than climate measures that vary at the pixel-year level. Third, world trends are not important for understanding particulates exposure during our sample period.

Table 4 shows that country level variation can explain close to half of all variation in exposure. We now investigate the importance of additional pixel level information. Table OA1 repeats variants of the population weighted regression of column 6 of table 4 where we add the following pixel-year level covariates one at a time, and all together: pixel-year population, our pixel-level urban indicator, and remotely-sensed measures of fires, share in crops, and share barren. These results require three comments.

First, all of the pixel level variables, except for fire, are highly significant when included singly or together. However, none of them does much to increase the precision with which we can estimate exposure. The R^2 for column 7 of table 4 is 0.56. Adding all of our pixel level covariates only increases this to 0.63. High quality, spatially disaggregated measures of particulate sources barely improve our ability to predict exposure once we know country-year of residence.

Second, the urban indicator variable reduces our prediction error by slightly more than does the linear term in population density, so the step function in density implied by the indicator variable is a better predictor of AOD than a linear function. The geography of our model is partly motivated by this finding. In our model, each country is divided into rural and urban regions.

Third, remotely-sensed measures of pixel share in crops and and barren are sources of dust, and unsurprisingly, contribute to exposure. Exposure is not purely anthropogenic. Physical geography plays a role. That our remotely-sensed measure of fire intensity is unimportant may seem surprising, but is consistent with the geography of smoke dispersion. Smoke plumes from wildfires often spread out over much larger areas than our 10km^2 pixels (Wen et al., (2023)).

We next investigate the extent to which pixel-year level variation in exposure can be attributed to country-year level variation in economic fundamentals. In table OA2, we present pixel level regressions of AOD on variables that vary only at the level of the country-year. These regressions are population weighted, and so measure the ability of particular country-year level variables to predict exposure.

The country level variables that we consider in table OA2 are measures of natural gas and renewables, coal, and petroleum per square kilometer of country area, and also GDP in services, industry and agriculture, also per unit of area. Holding mixing height constant, these variables are proportional to consumption per unit of country mixing volume. Because the physical process that determines concentration depends on particulate mass per unit volume, these normalized variables are more relevant to an investigation of concentration and exposure than unadjusted levels. We consider these variables both one by one and together.

Country-year level coal consumption has an R^2 of 0.14. Country-year level oil consumption and green power are both significantly related to equilibrium exposure, but have little predictive ability. The negative sign on green power moreover points to an inference problem that helps to motivate our model.[10]

Organic fuel consumption and agricultural burning per square km have the expected positive association with exposure and have even more ability to predict exposure than coal. GDP in services has little ability to predict exposure. Countries that produce more agricultural and industrial products have greater particulate exposure, although only agricultural GDP has much ability to predict exposure. Cross-border inflows increase exposure and conversely for outflows. These two variables have an R^2 of 0.04.

The final column of table OA2 includes all of these country-year level regressors together, and the results of this regression are important to our analysis. The R^2 of this regression is 0.39. In contrast, the R^2 in column 3 of table 4 (the comparable specification) is 0.46. That is, this relatively short list of likely suspects explains most of the variation in exposure that can be explained by factors that vary at the country-year level.

Finally, comparing table OA2 to table 2 we see that the regression results are broadly consistent with raw data describing emissions, although the raw emissions data suggests a relatively larger role for coal than do the regressions.

[10]While natural gas, wind, and solar power cause essentially zero particulate emissions, all else equal, they do not reduce concentration. More likely, countries that rely more heavily on these fuels also rely less heavily on dirtier power sources or regulate emissions more.

Our results so far suggest the following stylized facts about equilibrium exposure.

1. Exposure is substantially determined by country level factors. The importance of these factors is stable over time and substantially independent of climate.
2. Variation in exposure that is not explained by country-year factors is also not explained by a number of likely candidates that we measure at the pixel-year level.
3. Nearly all country-year level variation in exposure can be explained by a short list of economic fundamentals that vary at the country-year level.

In addition, the geography of exposure matters. India's exposure is dramatically lower than China's despite similar mean concentrations. These stylized facts jointly motivate the design of our model, which is described in the next section.

5. Model

This section presents the structure of our *Spatial Equilibrium Particulates Integrated Assessment* (SEPIA) model. Our goal is to use SEPIA to evaluate two classes of comparative statics: those that relate fossil energy and burning taxes to outcomes of immediate interest, exposure and welfare; and those that relate such levies to unintended consequences such as migration across regions or sectors. Both are of intrinsic and policy interest.

The model treats each country m as a small, open economy inhabited by a continuum of households. Each country contains two regions, urban (indexed by u) and rural (indexed by a). There are four sectors of production, summarized in table 5. We proceed by describing (i) production, (ii) households, (iii) government, (iv) the particulates model, and, finally (v) competitive equilibrium. Conventionally, we denote exogenous world prices with an "$*$" superscript, and let N_m represent country m's population size.

A *Production*

Industry: Industrial output, $Y_m^{I,k}$, in each region $k \in \{u,a\}$ in country m is produced using capital, $K_m^{I,k}$, labor, $L_m^{I,k}$, and composite energy, $J_m^{I,k}$. Energy is produced using coal, $E_{c,m}^{I,k}$, petroleum, $E_{p,m}^{I,k}$, and clean (green/natural gas), $E_{g,m}^{I,k}$, as inputs. We adopt a standard specification of technology (e.g., Golosov et al. (2014)):

$$Y_m^{I,k} = A_m^{I,k}(K_m^{I,k})^{\alpha}(L_m^{I,k})^{1-\alpha-v^I}\left(J_m^{I,k}\right)^{v^I} \tag{1}$$

$$J_m^{I,k} \equiv \left(\kappa_{c,m}^I(E_{c,m}^{I,k})^{\frac{\varepsilon-1}{\varepsilon}} + \kappa_{p,m}^I(E_{p,m}^{I,k})^{\frac{\varepsilon-1}{\varepsilon}} + \kappa_{g,m}^I(E_{g,m}^{I,k})^{\frac{\varepsilon-1}{\varepsilon}}\right)^{\frac{\varepsilon}{\varepsilon-1}}. \tag{2}$$

Competitive producers rent capital from international markets at price R^*, hire labor at the local wage w_m^k, and buy energy services at price $p_{J,m}^{I,k}$. The energy producers, in turn, import fuels at given prices (p_c^*, p_p^*, p_g^*). Polluting fuel use in all sectors may be subject to ad-valorem taxes $\tau_{c,m}$ and $\tau_{p,m}$. Industrial output serves as numeraire.

Services: Production of services, Y_m^S, is analogous to industry. Parameters differ so as to capture, e.g., greater importance of petroleum in services.

$$Y_m^S = A^S (K_m^S)^\alpha (L_m^S)^{1-\alpha-v^S} \left(J_m^S\right)^{v^S} \tag{3}$$

$$J_m^S \equiv \left(\kappa_{c,m}^S (E_{c,m}^S)^{\frac{\varepsilon-1}{\varepsilon}} + \kappa_{p,m}^S (E_{p,m}^S)^{\frac{\varepsilon-1}{\varepsilon}} + \kappa_{g,m}^S (E_{g,m}^S)^{\frac{\varepsilon-1}{\varepsilon}}\right)^{\frac{\varepsilon}{\varepsilon-1}}. \tag{4}$$

Services are not tradable and so their price p_m^S is domestically determined.

Agriculture: Agriculture Y_m^{Ag}, differs from the other sectors in two ways. First, we assume decreasing returns to scale to reflect unmodeled land inputs. Second, we model agricultural waste burning B_m and the cost $\Omega_m(\mu_m)$ of reducing fires by fraction μ_m:

$$Y_m^{Ag} = (1 - \Omega_m(\mu_m)) \cdot A_m^{Ag} (L_m^{Ag})^{\rho_{Lm}^{Ag}} (K_m^{Ag})^{\rho_{Km}^{Ag}} (J_m^{Ag})^{\rho_{Jm}^{Ag}}. \tag{5}$$

As is common, we assume that agricultural land rents $\pi_m^{Ag} \equiv ((1 - \rho_L^{Ag} - \rho_K^{Ag} - \rho_J^{Ag}) p^{Ag^*} Y_m^{Ag})$ are paid to absentee landlords abroad.

Similarly to carbon abatement costs in Nordhaus (2017), our model of fire abatement costs provides a reduced form description of the fact that agricultural burning can be reduced through reductions in production, substitutions of labor (e.g., Norgrove and Hauser (2015)), and of capital (e.g., Sidhu et al., 2015). Let ζ_m denote the country's baseline agricultural burning intensity. Net burning, B_m, and associated abatement costs are given by:

$$B_m = (1 - \mu_m)(\zeta_m Y_m^{Ag}) \tag{6}$$

$$\Omega_m(\mu_m) = v_{1m} \mu^{v_2}. \tag{7}$$

Farmers may be subject to an excise tax, $\tau_{B,m}$, on burning.[11] Otherwise, the sector is analogous to services and industry: Competitive producers hire workers in the rural labor market, rent capital from abroad, and obtain energy services based on an aggregator:

$$J_m^{Ag} \equiv \left(\kappa_{c,m}^{Ag} (E_{c,m}^{Ag})^{\frac{\varepsilon-1}{\varepsilon}} + \kappa_{p,m}^M (E_{p,m}^{Ag})^{\frac{\varepsilon-1}{\varepsilon}} + \kappa_{g,m}^M (E_{g,m}^{Ag})^{\frac{\varepsilon-1}{\varepsilon}}\right)^{\frac{\varepsilon}{\varepsilon-1}}, \tag{8}$$

[11] This tax serves as wedge representation of the different policies adopted in practice. For example, in India, farmers can be fined for crop residue burning (India Times, Nov. 17, 2018 "Despite Ban and Penalties, Stubble Burning Has Only Increased This Year").

Table 5: SEPIA Sectors

Sector	Location(s)	Tradeable?	Inputs
Industry (I)	Urban and Rural	Yes	Capital, Labor, Energy
Services (S)	Urban	No	Capital, Labor, Energy
Agriculture (Ag)	Rural	Yes	Capital, Labor, Energy
Energy Services ($J^k, k \in I,S,Ag$)	Urban and Rural	No	Coal, Oil, Gas/Green

Agricultural output is tradeable at the international price, p^{M^*}.

Emissions: Each sector in the model economy produces particulate emissions directly, and indirectly through energy consumption. Let ξ_m^z denote the particulate emissions intensity of activity z in country m. Industrial emissions in each location $k \in \{u,a\}$ may stem from (i) coal combustion $\xi_m^c E_{c,m}^{I,k}$, (ii) petroleum combustion $\xi_m^p E_{p,m}^{I,k}$, and (iii) process emissions (such as from iron and steel production) which we model as a by-product via $\xi_m^I Y_m^{I,k}$. Analogously, the services sector may contribute to urban particulate emissions through (i) coal combustion $\xi_m^c E_{c,m}^S$, (ii) petroleum combustion $\xi_m^p E_{p,m}^S$, and (iii) process emissions $\xi_m^S Y_m^S$ (such as road dust suspension from transportation). Finally, there are four sources of particulate emissions in the agricultural sector: (i) coal combustion $\xi_m^c E_{c,m}^{Ag}$, (ii) petroleum combustion $\xi_m^p E_{p,m}^{Ag}$, (iii) waste burning $\xi_m^B B_m$, and (iv) process emissions $\xi_m^{Ag} Y_m^{Ag}$ (such as fertilizer usage). Total endogenous particulate emissions, $Emiss^k$, in both regions are the sum of all emissions in the region,

$$Emiss_m^u \equiv \xi_m^c [E_{c,m}^S + E_{c,m}^{I,u}] + \xi_m^p [E_{p,m}^S + E_{p,m}^{I,u}] + \xi_m^S Y_m^S + \xi_m^I Y_m^{I,u} \tag{9}$$

$$Emiss_m^a \equiv \xi_m^c [E_{c,m}^M + E_{c,m}^{I,a,m}] + \xi_m^p [E_{p,m}^{Ag} + E_{p,m}^{I,a}] + \xi_m^{Ag} Y^{Ag} + \xi_m^I Y_m^{I,a} + \xi_m^B B_m. \tag{10}$$

B *Households*

The economy is populated by a continuum of households indexed by i. Households choose where to live and work based on their preferences over consumption, particulates, and an idiosyncratic net amenity value of living in the rural area, ϵ_i. This term captures the fact that urban-rural wage gaps often cannot be fully explained by observables, so that matching the data requires a residual preference for rural vs. urban areas (capturing, e.g., informal risk sharing networks).

Let c_m^j denote urban and x_m^j rural consumption of goods $j = I,S,Ag$, respectively. Utility is CES over the aggregate consumption bundle, which, in turn, is a Cobb-Douglas composite of the different consumption goods:

$$V_m^a(x_m^I, x_m^{Ag}, x_m^s, AOD_m^a, \epsilon_{i,m}) = \frac{\widetilde{x}_m^{1-\sigma}}{1-\sigma} - \chi_{1,m}(AOD_m^a)^{\chi_2} + \epsilon_{i,m} \tag{11}$$

$$\widetilde{x_m} \equiv (x_m^I)^{\theta_m^I}(x_m^S)^{\theta_m^S}(x_m^{Ag})^{1-\theta_m^I-\theta_m^S} \tag{12}$$

$$V_m^u(c_m^I, c_m^{Ag}, c_m^S, AOD_m^u) = \frac{\widetilde{c_m}^{1-\sigma}}{1-\sigma} - \chi_{1,m}(AOD_m^u)^{\chi_2} \tag{13}$$

$$\widetilde{c_m} \equiv (c_m^S)^{\theta_m^S}(c_m^I)^{\theta_m^I}(c_m^{Ag})^{1-\theta_m^I-\theta_m^S}. \tag{14}$$

Households supply one unit of labor inelastically[12] wherever they live, earning w_m^u in the urban area or w_m^a in the rural area. Households may receive lump-sum transfers T_m from the government. We abstract from households' savings and investment decisions. The annual budget constraints for households in each region are,

$$c_m^I + p_m^S c_m^S + p^{Ag^*} c_m^{Ag} \leq w_m^u + T_m \tag{15}$$

$$x_m^I + p_m^S x_m^S + p^{Ag^*} x_m^{Ag} \leq w_m^a + T_m. \tag{16}$$

Because the manufactured good is the numeraire in both regions, we are implicitly assuming that trade in this good across the two regions is costless.

Free mobility implies that a marginal household will be just indifferent between living in the urban or rural area. Their cutoff amenity value ϵ^* is thus defined by the condition:

$$\epsilon_m^* = \{\frac{\widetilde{c_m}^{1-\sigma}}{1-\sigma} - \chi_{1,m}(AOD_m^u)^{\chi_2}\} - \{\frac{\widetilde{x_m}^{1-\sigma}}{1-\sigma} - \chi_{1,m}(AOD_m^a)^{\chi_2}\}. \tag{17}$$

For our calibration exercise, ϵ_i follows a generalized extreme value distribution described in the appendix.

C *Government*

Our benchmark analysis considers the equilibrium impacts of both energy input taxes and agricultural burning taxes. Government revenue from these levies, G_m, is either discarded or re-distributed to households via lump-sum transfers T_m. We thus abstract from broader fiscal policy and posit the following public budget constraint:

$$G_m = \tau_{B,m}B_m + \tau_{c,m}\sum_j E_{c,m}^j + \tau_{p,m}\sum_j E_{p,m}^j,\ j \in \{I,a; I,u; S; Ag\} \tag{18}$$

$$N_m \cdot T_m \leq G_m$$

[12]We thus abstract from air quality impacts on labor supply as in Hanna and Oliva (2015).

D *Pollution Model*

To describe the way that particulates are transported across boundaries, we rely on a two box diffusion model, a slight generalization of an elementary particulate transport model.[13] Such stylized box-diffusion models are common in the integrated assessment literature, e.g., the global carbon cycle (e.g., Nordhaus (2017)).

In our model, there are three regions, a box for the rural region, a box for the urban region, and the rest of the world. Inflows from the rest of the world are exogenous. The model's four main assumptions are: particulates are uniformly dispersed within each box; the mass of particulates is conserved; the system is in steady state; and the deposition rate of particulates in each box is proportional to the total mass in the box.[14]

So far, we have partitioned countries into rural and urban regions. For the purpose of describing particulate transport we instead consider a sending region and a receiving region, where the sending region is a net exporter of particulates to the receiver. Index these regions by $k \in \{s,r,w\}$. We omit country subscripts m here for legibility.

Figure 2 illustrates the main features of the particulate model. Each region $k \in \{s,r\}$ contains emissions sources that produce mass F^{kk} of particulates per unit of time (kg/year). Each region also receives a flow of particulates from the world, F^{wk}, and sends a flow of particulates to the rest of the world, F^{kw}. The sending region also sends F^{sr} to the receiver. Deposition, or "flow into the ground", is denoted D^k.

In any steady state, the conservation of mass requires the sum of flows in and internal sources must equal the sum of deposition and flows out,

$$\begin{aligned} 0 &= F^{ss} - D^s + F^{ws} - F^{sw} - F^{sr} \\ 0 &= F^{rr} - D^r + F^{wr} - F^{rw} + F^{sr}. \end{aligned} \tag{19}$$

The first of these two equations gives a mass balance condition for the sending region, and the second for the receiving region. The two conditions are symmetric except for the treatment of flows from s to r.

[13]For example, Jacob (1999b). We note that detailed pollution dispersion models have been developed for both regulatory and research purposes (e.g., EPA (2017)). However, these models are typically designed for the analysis of specific sources' impacts at fine spatial and temporal scales. The goals of this paper, in contrast, are (i) to study pollution movement and concentration changes over large spatial (two regions per country) and temporal (annual) scales, and (ii) to integrate a representation of these processes with a macroeconomic model. These considerations favor our approach.

[14]Perfect dispersion within each box is a simplifying assumption, and without this assumption the problem rapidly becomes intractable. The conservation of the mass of particulates is a basic physical principle and requires that particulates in each box reflect the net of sources, flows in, deposition, and flows out. Our focus on steady state equilibrium is also a simplifying assumption, but one that appears well grounded. We are interested in annual averages, while, as we saw in table 2, the deposition, flow and production of particulates operates over much shorter time scales.

We next describe the components of equation (19). For $k,k' \in \{s,r,w\}$, introduce the following notation. Let $l^{kk'}$ be the length in km of the border over which wind blows from k to k' (km) for $k,k' \in \{s,r,w\}$ and let $v^{kk'}$ be the mean annual wind velocity across this border (km/yr). Let AOD^k be AOD in region k and A^k be the area in km^2 of this region. Emiss^k is particulate emissions in region k (kg/year) from modeled economic activities and $Emiss_{EX}^k$ is particulate emissions from unobserved sources such as dust. Finally, λ is the common mixing height (km) and ρ the AOD to PM10 conversion factor (kg/km^3 per AOD unit).

The $Emiss^k$ are exactly the quantities defined in equations (9) and (10). However, we here index anthropogenic emissions by their sender or receiver status when we earlier indexed them by whether they described rural or urban regions. We are actually describing two distinct economic models, one in which the sending region is urban and another in which it is rural. In our calibrations, we will choose between these two models on the basis of the case that obtains for each particular country in the data.

We can describe the components of equation (19) as follows. The flow into and out of each region $F^{kk'}$ is the product of the concentration of particulates in the source region times the volume of air that crosses from the source into the sink region. For $k,k' \in \{w,s,r\}$ and $k \neq k'$, we have

$$F^{kk'} = v^{kk'} \lambda l^{kk'} \rho \text{AOD}^k. \tag{20}$$

The first three terms calculate the volume of air crossing the kk' border in a year, and the last two terms give the upwind concentration of PM10. The product of volume and concentration is the mass of particulates transported from k to k'.

Next, given area, A^k, the AOD to PM10 conversion factor, ρ, and the deposition velocity, v_D^k, deposition is given by,

$$D^k = v_D^k A^k \rho \text{AOD}^k, \tag{21}$$

for $k \in \{s,r\}$. Flow across the border reflects flow across the area λl^{kw} at velocity v^{kw}. Deposition reflects flow into land area A^k at velocity v_D^k.

Finally, emissions in each region are given by:

$$\begin{aligned} F^{ss} &= Emiss^s + Emiss_{EX}^s \\ F^{rr} &= Emiss^r + Emiss_{EX}^r \end{aligned} \tag{22}$$

Substituting (20)-(22) into (19) and rearranging yields expressions for equilibrium AOD in each region:

Figure 2: A Two-Box model of particulate concentration

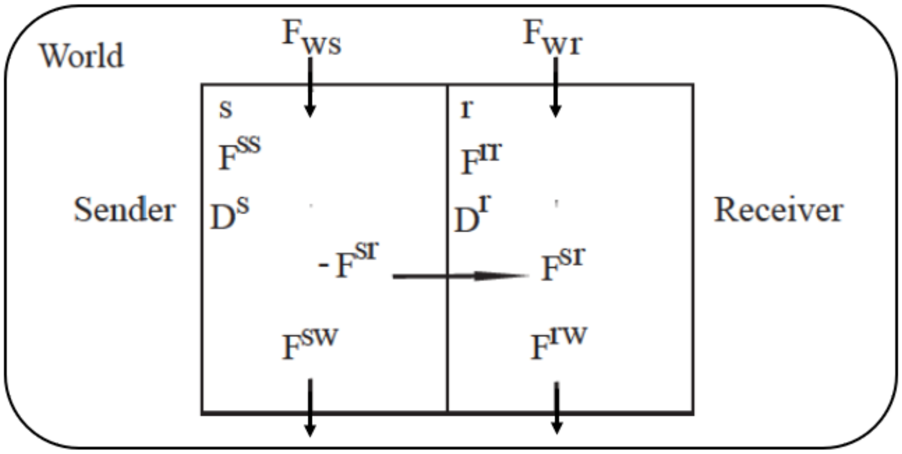

Note: *Illustration of two-box model of particulate flows between sending and receiving region and the rest of the world. F^{sr} is flow from sender to receiver. F^{sw} and F^{rw} are flows from sender and receiver to the world. F^{ws} and F^{wr} are flows from the world to the sender and receiver. F^{ss} and F^{rr} are emissions. D^s and D^r are deposition.*

$$AOD^s(Emiss^s) = \frac{v^{ws}\lambda l^{ws}\rho AOD^w + Emiss^s_{EX}}{\rho\left[v^s_D A^s + \lambda(v^{sw}l^{sw} + v^{sr}l^{sr})\right]} + \frac{Emiss^s}{\rho\left[v^s_D A^s + \lambda(v^{sw}l^{sw} + v^{sr}l^{sr})\right]} \tag{23}$$

$$\begin{aligned} AOD^r(Emiss^s, Emiss^r) = {} & \frac{v^{wr}\lambda l^{wr}\rho AOD^w + Emiss^r_{EX}}{\rho(v^r_D A^r + v^{rw}\lambda l^{rw})} + \frac{Emiss^r}{\rho(v^r_D A^r + v^{rw}\lambda l^{rw})} \\ & + \frac{v^{sr}\lambda l^{sr}}{v^r_D A^r + v^{rw}\lambda l^{rw}} AOD^s(Emiss^s). \end{aligned}$$

E *Competitive Equilibrium*

Competitive equilibrium consists of an allocation $\{L^{I,u}_m, L^{I,a}_m, L^S_m, L^{Ag}_m;\ K^{I,u}_m, K^{I,a}_m, K^S_m, K^{Ag}_m;\ J^{I,u}_m, J^{I,a}_m, J^S_m, J^{Ag}_m;\ E^{I,u}_{c,m}, E^{I,u}_{p,m}, E^{I,u}_{g,m},\ E^{I,a}_{c,m}, E^{I,a}_{p,m}, E^{I,a}_{g,m},\ E^S_{c,m}, E^S_{p,m}, E^S_{g,m},\ E^{Ag}_{c,m}, E^{Ag}_{p,m}, E^{Ag}_{g,m};\ x^I_m, x^{Ag}_m, x^S_m;\ c^I_m, c^{Ag}_m, c^S_m;\ B_m, \mu_m, AOD^u_m, AOD^a_m\}$ a set of prices $\{p^S_m, p^{I,u}_{J,m}, p^{I,a}_{J,m}, p^S_{J,m}, p^{Ag}_{J,m};\ w^u_m, w^a_m\}$ and policies $\{\tau^j_{c,m}, \tau^j_{p,m}, \tau_{B,m}, T\}$ for $j \in \{I,a; I,u; S,Ag\}$ such that: (1) Profits are maximized in each sector given prices and policies; (2) Household utility is maximized in each location given prices; (3) Markets for labor and the domestic services clear:

$$N_m = L^{I,u}_m + L^{I,a}_m + L^S_m + L^{Ag}_m \tag{24}$$

$$Y^S_m = c^S_m(L^S_m + L^{I,u}_m) + x^S_m(L^{Ag}_m + L^{I,a}_m); \tag{25}$$

(4) Budget constraints of the government (18) and the nation are satisfied:

$$(L_m^M + L_m^{I,a})(x_m^I + p^{Ag^*} x_m^{Ag}) + (L_m^S + L_m^{I,u})(c_m^I + p^{Ag^*} c_m^{Ag}) + p_c^* \sum_j \{E_{c,m}^j\} + p_p^* \sum_j \{E_{p,m}^j\} + p_g^* \sum_j \{E_{g,m}^j\}$$
$$+ R^*(K_m^{I,u} + K_m^{I,a} + K_m^S + K_m^{Ag}) + \pi_m^{Ag} + (G_m - N_m \cdot T_m) \le Y_m^{I,u} + Y_m^{I,a} + p^{Ag^*} Y_m^{Ag}; \tag{26}$$

(5) AOD obeys the laws of nature (23) and (9)-(10). The Online Appendix provides details of these conditions for the functional forms of our model.

6. Calibration

Calibration proceeds in three steps. First, we set values for "directly calibrated" parameters at common values for all countries based on the literature or standard assumptions. Second, we back out many parameter values directly from data for each country ("directly from data"). Third, we select the remaining model parameters to jointly minimize the sum of squared differences between equilibrium moments as observed in the data and our model for each country ("matching moments"). We here discuss key data sources and parameters. The Appendix provides more detail.

Production and energy: For each country m we observe sectoral output values. Using a tilde to distinguish between revenues and quantities, we observe ($\widetilde{Y_m^I} \equiv Y_m^I$, $\widetilde{Y_m^{Ag}} \equiv p^{Ag^*} Y_m^{Ag}$, $\widetilde{Y_m^S} \equiv p_m^S Y_m^S$) directly from the World Bank, the initial distribution of labor across urban and rural areas from GPW, and energy inputs at the fuel-sector level (e.g., petroleum used in agriculture in Bangladesh in 2010) from the International Energy Agency (IEA). The fuel share parameters for energy production in each country-sector (e.g., $\kappa_{p,m}^{Ag}$) can then be inferred directly from optimality conditions (OA4)-(OA5) by using data on fuel prices (from British Petroleum Company (2016)) and substitution elasticities (ε) calibrated based on prior literature (see Appendix). For the parameters of sectoral production, we solve for the initial equilibrium to obtain unobserved prices (e.g., rural and urban wages) and infer the initial distribution of industrial production in urban and rural areas. Intuitively, we use the initial observed distribution of the population across regions, along with observed regional AOD, aggregate data moments (e.g., total industrial output), and our model equilibrium conditions to infer this distribution via joint matching of moments (see Appendix). Finally, we quantify agricultural burning abatement costs based on each country's baseline residue burning intensity and crop mix, along with estimates from the literature (see Appendix).

Households: Preferences over consumption goods are country-specific and are estimated from World Bank data on sectoral household expenditures (2010) and services sector output shares. Calibration of preferences over AOD and rural living is more challenging. The benchmark calibration sets particulates disutility level parameter $\chi_{1,m}$ to match empirical estimates of household willingness to pay (WTP) for particulate reductions by Ito and Zhang (2019). Ito and Zhang (2019) estimate a mean WTP of USD 5.46 per $\mu g/m^3$ PM10 reduction for households in China with an annual income of $2,253 who experience mean winter PM10 concentrations of 115 $\mu g/m^3$. We assume a quadratic particulates disutility curvature (χ_2=2) and set $\chi_{1,m}$ to match this WTP estimate given each country's consumption preferences and domestic price levels.[15]

Given these preference parameters, we can then infer the equilibrium rural amenity value ϵ_m^* for the marginal household by using the free mobility condition (17). Our generalized extreme value distribution assumption necessitates the selection of shape, scale, and location parameters, which we jointly select to match (i) each country's observed base year distribution of the population given relative wages and particulates levels, (ii) a benchmark migration-wage elasticity estimate of 1.9 from Morten and Oliveira (2018), and (iii) the standard location parameter percentile (see Appendix for details).

Particulates: The baseline particulates intensities of different fuels and activities, the ξ's in (9)-(10), can differ markedly across countries. To quantify these parameters, we use country- and activity-specific PM10 particulate intensity estimates from the IIASA GAINS model. IIASA collects and processes detailed data on countries' fuel input mixes (e.g., ash content of coal), technologies (e.g., the distribution of boiler types), and considers baseline environmental policy and mandated abatement levels to construct country-, year- and activity-specific estimates of emissions factors.

For the particulates dispersion model, we observe area, boundary, and wind information directly in our geographical and meteorological data. We obtain rural and urban specific estimates of deposition velocity from the EPA's ASPEN model (Assessment System for Population Exposure Nationwide, EPA (2000)).[16] Average mixing height, λ, is estimated based on data from the EPA's Support Center for Atmospheric Modeling, and we set the AOD-PM10 conversion parameter, ρ, at 100 $\mu g/m^3$ based on Gendron-Carrier et al. (2022). Finally, we set exogenous emissions, $Emiss_{EX,m}^k$, in each country-region-year as the residual to match observed AOD levels.

[15] Ito and Zhang's estimates represent a 5-year aggregate. We convert this figure into an annualized equivalent assuming a personal discount rate of 3% per year.

[16] The ASPEN model is a detailed pollution dispersion framework developed by the US EPA. It considers annual averages of pollution dispersion, as required for our framework.

Figure 3: Changes in exposure from emissions policies (%)

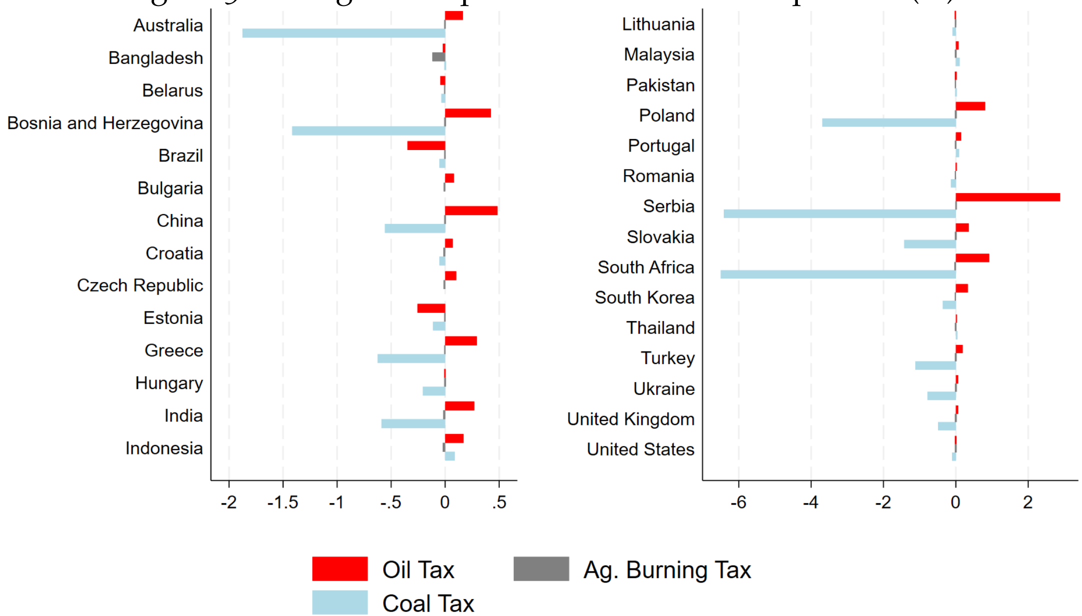

(a) No Transfers

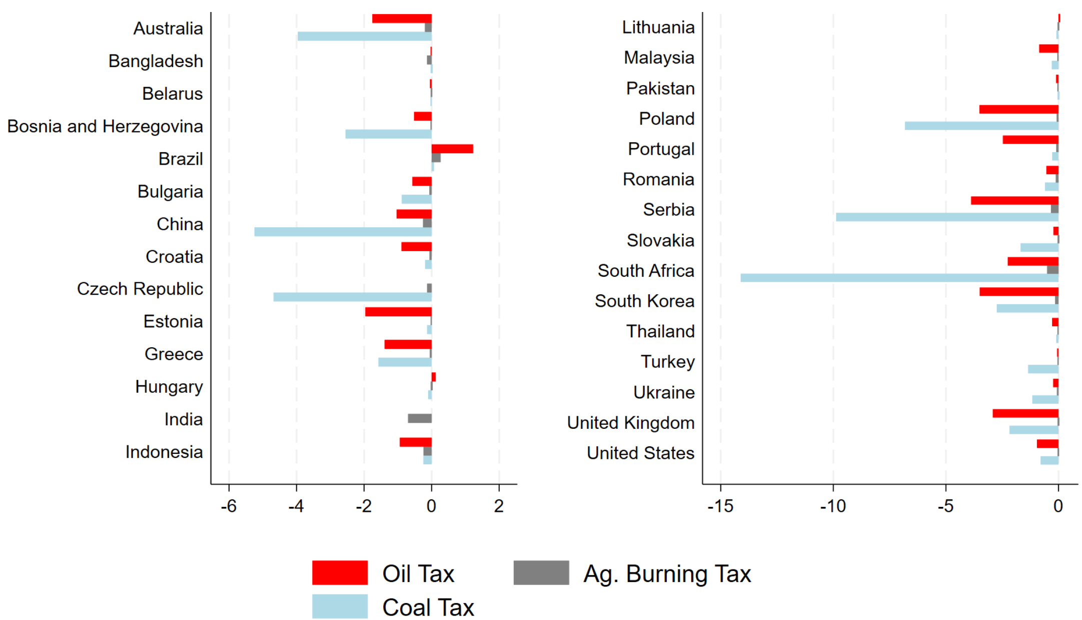

(b) With Transfers

Note: *All panels' x-axes show the percentage change in aggregate particulate exposure from each policy (10% tax on oil, 15% tax on coal, 30\$/MT tax on agricultural burning) in each country. Panel (a) assumes tax revenues are discarded. Panel (b) assumes revenues are rebated lump-sum to households.*

7. Counterfactual policy evaluation

We here describe the results of the policy experiments for the roughly [17] 30 countries for which the data permit calibration and counterfactual analysis.

We consider three policies: A 10% ad-valorem tax on petroleum inputs, a 15% ad-valorem coal tax, and a \$30/MT unit tax on agricultural burning.

Panel (a) of figure 3 shows the predicted changes in national particulate exposure for each policy-country pair under the assumption that policy revenues are used for non-productive purposes. First, for the oil tax, prediced impacts range from -0.35% (in Brazil) to +2.9% (in Serbia). Strikingly, the results suggest that uncompensated oil taxes *increase* particulate exposure in the majority of model countries. For the agricultural burning tax, changes in exposure are generally small. For the coal tax, exposure decreases in most countries, but ranges from -6.5% (in South Africa) to +0.1% (in Malaysia).

We next illustrate the mechanisms underlying these aggregate results using South Africa as an example. Table 6 shows that the (uncompensated) oil tax is predicted to *increase* aggregate particulates exposure by around 1% despite the fact it decreases oil use by more than 10% in both rural and urban areas. This occurs because South African agriculture relies heavily on oil as energy input,[18] leading to a decline in agricultural output and employment as a result of the oil tax. The displaced workers move to more polluted urban areas and the heavily coal-based urban industrial sector. This increases both migrant exposure and urban particulates. Similarly, while the agricultural burning tax is predicted to reduce burning emissions by 15%, it also causes a decline in agricultural output and employment. Here, displaced workers shift mainly into rural industry, leading to a small increase in rural coal use but on net also a small aggregate decrease in particulates exposure. Finally, coal taxes lead to substantial declines in both urban and rural particulates exposure. In sum, we find that general equilibrium effects can substantially undermine the direct *emissions* reduction benefits of particulate policies.

We further illustrate this point by comparing predicted changes in equilibrium *exposure* to the predicted ceteris paribus effects based on changes in targeted *emissions*. For each tax, we weight the predicted changes in emissions from the targeted activity by its baseline share of total emissions. For example, if the coal tax decreased coal emissions by 20%, and if coal accounted for 50% of total emissions in the baseline, we calculate a 20%

[17] In a handful of country-policy pairs the counterfactuals did not converge within the precision required by our analysis, leaving us with less than 30 countries.

[18] In 2010, oil accounted for 64% of final energy use in South Africa's agriculture sector, compared to, e.g., 2% in manufacturing (IEA). More recent numbers are similar (e.g., 68% vs. 2% in 2022).

Table 6: Counterfactual results for South Africa in base year 2010 with policy revenue discarded.

Panel A: Overall Impacts

	Agg. Exposure (AOD×bil.)	Agg. Exposure %Δ	Urban Pop. Share	Urban Exposure %Δ	Rural Exposure %Δ	Agg. Welfare %Δ
Baseline	0.00424	-	0.62	-	-	-
Oil Tax	0.00428	0.92	0.63	1.87	-0.79	-0.15
Burning Tax	0.00424	-0.04	0.62	-0.01	-0.10	0.00
Coal Tax	0.00396	-6.50	0.64	-6.65	-6.22	-1.19

Panel B: Rural Impacts

	Industry Output ($bil.)	Industry Empl. (bil.)	Ag. Output ($bil.)	Ag. Empl. (bil.)	Ag. Burning (MT)	Coal Use (ktoe)	Oil Use (ktoe)	AOD
Baseline	53.2	0.015	1471.6	0.004	5.3	24.1	1.6	0.083
Oil Tax	53.3	0.015	1406.3	0.003	5.1	24.2	1.3	0.083
Burning Tax	55.1	0.015	1276.5	0.003	4.5	24.4	1.5	0.083
Coal Tax	47.0	0.013	1590.8	0.004	5.7	18.6	1.8	0.082

Panel C: Urban Impacts

Policy	Industry Output ($bil.)	Industry Empl. (bil.)	Services Output (units)	Services Empl. (bil.)		Coal Use (ktoe)	Oil Use (ktoe)	AOD
Baseline	122.9	0.007	2158.2	0.023		82.6	17.6	0.091
Oil Tax	123.9	0.008	2158.8	0.023		85.1	15.3	0.092
Burning Tax	122.9	0.007	2158.2	0.023		82.6	17.6	0.091
Coal Tax	128.3	0.008	2184.2	0.023		71.0	18.9	0.082

Note: *Each panel reports outcomes in four cases, baseline, with an oil tax, a tax on agricultural burning, and a coal tax. The top panel reports country level statistics. The middle panel reports outcomes for rural areas, and the bottom panel reports on the urban area. Exposure is measured in AOD times population in billions.*

· 50% = 10% reduction in aggregate pollution. This calculation is a partial equilibrium estimate of the reduction in particulate burdens.

Figure 4 compares the change in emissions and exposure for six countries. This figure again shows the importance of this distinction. As expected, emissions fall in response to regulation. However, for agricultural burning restrictions and oil taxes, the magnitude of the change in emissions is often much larger than the change in exposure. Burning restrictions reduce agricultural burning emissions, but also push workers out of farming into rural industry or more polluted urban areas, and this offsets the direct benefits. Given the agricultural sector's disproportionate reliance on oil in many countries, similar effects occur with oil taxes. Income lost to oil taxes incentivizes migration to higher wage urban areas. In some cases, the offsetting effects are larger than the direct effect and the

Figure 4: Emissions vs. exposure with policy revenue discarded.

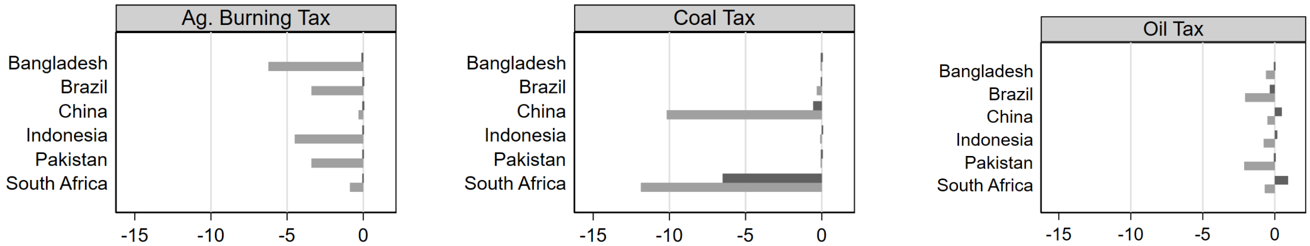

(a) Ag. burning tax (b) Coal tax (c) Oil tax

Note: *The x-axis in all three panels indicates percentage change. Dark gray indicates percentage change in country mean particulate exposure resulting from each policy. Light gray indicates percentage change in country aggregate emissions. The three panels describe, from left to right, an agricultural burning tax of 30\$/MT, a 10% tax on oil, and a 15% tax on coal. Tax revenue is discarded in every case.*

change in emissions has a different *sign* than the change in exposure. Figure 4 also shows the importance of cross-country heterogeneity. Even when using the same model structure to compare outcomes across countries, both the estimated policy impacts and the gap between partial and general equilibrium outcome measures differs in magnitude and in *sign* across countries. For example, unlike the other countries considered in figure 4, in Brazil particulates are on average lower in urban areas and oil taxes decrease exposure by *more* than emissions.

The results also showcase the importance of income support. We so far assumed that policy revenues are spent non-productively. Panel (b) of figure 3 describes the effects of policy on exposure when tax revenues are instead rebated to households lump-sum. The results indicate that *combining particulate policies with income support dramatically increases their effectiveness for most countries and policies*: coal tax impacts now more than double for several countries (up to -14% in South Africa), oil tax impacts are now mostly negative, and agricultural burning taxes reduce exposure (up to -0.7% in India).

Table OA3 again illustrates the underlying intuition by presenting detailed results for South Africa as in table 6 but with lump-sum revenue rebating. All policies appear more effective at reducing aggregate particulates exposure. This difference is largely due to the fact that helping rural households make up for the real income losses associated with each policy helps avoid their movement to the (typically more polluted) cities and sectors, as can be seen from the higher rural population shares with revenue-rebating.

Table 7 further illustrates the importance of both income support and cross-country heterogeneity. This table compares policies' welfare-rankings in six countries. Specifically, we compare policies' impacts on aggregate utility in each country, and rank them from best (rank 1) to worst (rank 3). Two features of table 7 stand out. First, each policy ranks highly in some countries but poorly in others. Second, rankings may depend

Table 7: Policy welfare rankings across countries

	No Lump-Sum Rebate			Lump-Sum Rebate		
	Ag. Burning	Coal	Oil	Ag. Burning	Coal	Oil
Brazil	1	2	3	2	3	1
China	1	3	2	3	1	2
Pakistan	1	2	3	2	3	1
Bangladesh	2	3	1	2	2	1
Indonesia	1	2	3	2	3	1
South Africa	1	3	2	3	2	1

Note: *This table shows the welfare ranking of three policies by country; an agricultural burning tax of 30$/MT, for a 10% tax on oil, and a 15% tax on coal. The first three columns describe the way these policies are ranked when tax revenues are discarded. The second three columns describe the way policies are ranked when tax revenues are rebated lump sum.*

on revenue management. For example, in Pakistan, the oil tax ranks worst (3) when revenues are discarded, but ranks best (1) when revenues are rebated lump-sum.

Three main insights emerge from the quantitative analysis. First, the results highlight the first-order importance of considering tax impacts on pollution *exposure*. That is, understanding policy impacts on *emissions* may be insufficient to predict their effects on exposure. For example, oil taxes reduce particulate emissions from oil combustion and complementary activities, but the associated general equilibrium responses may pushe workers into more polluting activities or regions. We also find examples where such adjustments magnify the benefits of a tax, consistent with the empirical evidence showing that countries' changes in exposure can be substantially larger or smaller than their changes in concentrations.

Second, the results demonstrate the importance of national context for the assessment of policy. An apples-to-apples comparison based on the same analytic framework shows that the same fossil energy tax can have *qualitatively* different impacts on exposure and welfare in different countries.

Third, the results highlight the importance of fiscal policy for the effectiveness of particulates policy. Because income transfers affect household location decisions, the same policy can have *qualitatively* different impacts on exposure depending on whether tax revenues are redistributed. While a large literature has demonstrated the importance of revenue recycling for the efficiency and distributional impacts of climate policy (see, e.g., Goulder and Hafstead (2018), Metcalf (2018), Barrage (2019), Conte et al. (2025)), to the best of our knowledge the finding of *qualitatively* different environmental effects depending on rebating is novel.

8. Sensitivity analysis

We now evaluate the sensitivity of our results to five key parameters: AOD disutility, the migration-wage elasticity, atmospheric mixing height, agricultural burning abatement costs, and the elasticity of substitution across energy inputs. For each triplet of *parameter* $\times$ *policy experiment* $\times$ *country*, we compare the predicted effects of the policy on exposure in the benchmark (no rebates) to an alternative calibration where the parameter in question is increased by +1%. For example, we re-compute the effects of an agricultural burning tax in each country with the AOD disutility 1% higher than in the benchmark, and calculate the change in the aggregate exposure effect prediction for each country. Figure 5 displays the results of these experiments via box plots of the distribution of these quasi-elasticities across countries. Analogous results for the scenarios with income transfers are shown in the Online Appendix.

We find that the model's results are mostly insensitive to changes in the assumed AOD disutility[19] and mixing height. The agricultural burning tax results are sensitive to our assumptions about fire abatement costs, the oil tax results are sensitive to the migration-wage elasticity, and both the oil and coal tax results show some sensitivity to the fuel substitution elasticity. Interestingly, the sensitivity cannot be signed and varies qualitatively across countries. These results highlight the importance of empirical research to improve our understanding of the costs of agricultural burning mitigation (e.g., Jack, Jayachandran, Kala, and Pande (2025)), migration responsiveness to wages (e.g., Morten and Oliveira (2018)), and the elasticity of substitution across energy inputs in production (e.g., Papageorgiou, Saam, and Schulte (2017)) across countries.

9. Conclusion

Fossil fuel levies and subsidies are among the most widely applied excise taxes in the world (OECD 2019; IEA 2023). And while the argument is frequently made that increasing net prices on fossil fuels would create substantial value by reducing air pollution emissions (e.g., Parry et al. 2014; WB 2021), relatively little is known about how such policies might affect aggregate particulate exposure in (spatial) equilibrium. The stakes in understanding these effects are large as ambient particulate exposure remains a leading global risk factor for premature mortality (GBD 2024).

[19]The alternative calibration with higher AOD disutility also re-calculates the distribution parameters of the rural amenity value as required to match the initial population distribution and assumed migration-wage elasticity. This may offset some of the ceteris paribus migration effects of higher AOD disutility.

Figure 5: Sensitivity Analysis: Level Change in Exposure per 1% Change in Parameter

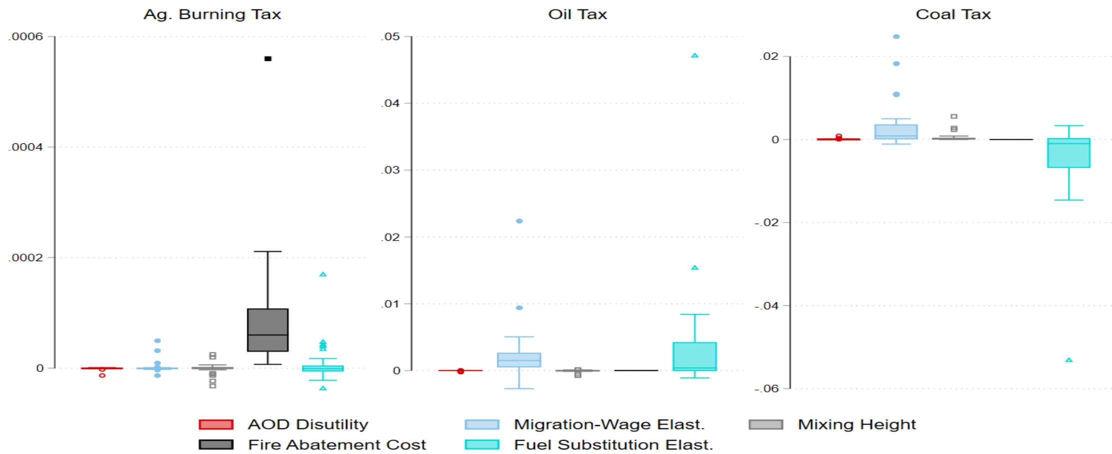

Note: *Sensitivity of results to five key parameters: AOD disutility, the migration-wage elasticity, atmospheric mixing height, agricultural burning abatement costs, and the elasticity of substitution across energy inputs. For each triplet of parameter × policy experiment × country, we compare the predicted effects of the policy on aggregate particulate exposure in the benchmark (no rebates) to an alternative calibration where the parameter in question is increased by +1%. The figure describes the results of these experiments with box plots of the distribution of the percentage point difference in predicted exposure effects. The box spans the 25th-75th percentile, the line represents the median, and the whiskers represent 1.5 times the inter-quartile range.*

This paper contributes to this debate in three parts. First, we assemble gridded panel data of particulate concentrations and population throughout the world. The data demonstrate the importance of considering *exposure* as an outcome: Countries' changes in particulate *concentrations* can be substantially larger or smaller than their changes in aggregate exposure. Intuitively, this is because the same processes that change pollution levels also affect where pollution occurs relative to populations.

Second, we use the data to inform the design of a new macroeconomic particulates integrated assessment model. Empirically, we find that (i) almost half of all pixel-level variation in exposure is captured by country fixed effects; (ii) most country-year level variation in exposure is explained by a tractable number of country-year economic variables; urbanization, coal and oil consumption, agricultural GDP and residue burning, organic fuel consumption, and cross-border particulate flows; (iii) perhaps surprisingly, the half of variation in exposure that is not explained by country-year fixed effects is also not explained by pixel-level variables; population density, land cover and fires. We take from these results the importance of country-level factors, of modeling different economic sectors and fuel inputs, of spatially capturing urban vs. rural populations and production, and of accounting for particulate dispersion within and across countries.

Third, in order to evaluate the counterfactual effects of fossil energy taxes and agricultural residue levies, we develop such a model (SEPIA). We quantify the model using detailed country-level information such as on fuel use by country-sector and particulate emissions factors by country-activity. Calibrating this model for 30 countries allows us to evaluate tax impacts on a country-by-country basis.

The model results highlight three main points. First, uncompensated oil and agricultural burning taxes may fail to reduce or even increase equilibrium particulate *exposure* despite decreasing targeted activity *emissions*. This discrepancy arises precisely because these taxes shift workers to more polluted areas and/or sectors. Second, both policies become significantly more effective if coupled with income support (lump-sum rebates) which reduces pressure on workers to shift locations. Third, coal taxes appear broadly effective at reducing particulate exposure: even our 15% ad valorem tax - equivalent to a carbon price of <$10/tCO2 - is projected to change exposure by up to -14% (in South Africa), with large reductions also in Serbia, Poland, China, and Australia. While fossil fuel taxes thus clearly hold the potential to generate large co-benefits even in (spatial) equilibrium, reductions in emissions are not sufficient to ensure reductions in exposure.

A good deal of research remains to be done. First, our primary unit of analysis is an annual average over a 10km^2 pixel. In contrast, much of the research on particulates considers much smaller spatial scales and shorter time frames. Our relatively aggregated measure is smoothing out variation in particulate exposure that may be economically important, but is beyond the reach of our data. Second, our object is to develop a model that would allow us to evaluate policy relevant comparative statics across countries. This requires that we satisfy ourselves with a stylized description of each county's economy. It is clearly feasible to develop country specific models that provide a more detailed description of equilibrium particulate exposure, as illustrated by, e.g., Hollingsworth et al. (2024) for the USA. While this nascent literature has not considered fossil fuel taxes, we hope that our work precipitates more studies in this line of research. Such work could also combine the richer spatial economic representations of the climate literature (as in, e.g., Cruz and Rossi-Hansberg (2024)) with the detailed energy system and multi-sector economic representation of the SEPIA model to study particulate pollution. Third, our analysis abstracts from secondary particulate pollution. Accounting for additional pollutants and their interactions with particulates would thus be another important direction for future work.

Finally, our work highlights the importance of more empirical evaluations of the real-world impacts of fossil fuel prices on particulate exposure. For concentrations, this nascent literature already suggests mixed results, with particulate reductions from, e.g., higher fuel taxes observed in Germany (Basaglia et al. 2023) but not in Iran (Kheiravar and Lawell 2020). Understanding whether, when, and why conventional tax instruments reduce population exposure - rather than emissions or concentrations alone - thus remains a critical research challenge.

References

Joseph E. Aldy, Maximilian Auffhammer, Maureen Cropper, Arthur Fraas, and Richard Morgenstern. Looking back at 50 years of the clean air act. *Journal of Economic Literature*, 60(1):179–232, 2022.

Eva Arceo, Rema Hanna, and Paulina Oliva. Does the effect of pollution on infant mortality differ between developing and developed countries? evidence from Mexico City. *The Economic Journal*, 126(591):257–280, 2016.

Lint Barrage. Optimal dynamic carbon taxes in a climate-economy model with distortionary fiscal policy. *Review of Economic Studies*, 2019.

Piero Basaglia, Sophie M Behr, and Moritz A Drupp. De-fueling externalities: Causal effects of fuel taxation and mediating mechanisms for reducing climate and pollution costs. 2023.

Piero Basaglia, Jonas Grunau, and Moritz A Drupp. The european union emissions trading system might yield large co-benefits from pollution reduction. *Proceedings of the National Academy of Sciences*, 121(28):e2319908121, 2024.

Simon Black, Weronika Celniak, Alberto Garcia-Huitrón, Ian Parry, Paulina Schulz Antipa, and Nate Vernon-Lin. Underpriced and overused: Fossil fuel subsidies data 2025 update. IMF Working Paper WP/25/270, International Monetary Fund, Washington, DC, 2025. URL `https://www.imf.org/-/media/files/publications/wp/2025/english/wpiea2025270-source-pdf.pdf`.

Brauer et al. Ambient air pollution exposure estimation for the global burden of disease 2013. *Environmental Science & Technology*, 50(1):79–88, 2015.

British Petroleum Company. BP statistical review of world energy. https://www.bp.com/en/global/corporate/energy-economics/statistical-review-of-world-energy.html, 2016.

Michał Burzyński, Christoph Deuster, Frédéric Docquier, and Jaime De Melo. Climate change, inequality, and human migration. *Journal of the European Economic Association*, 20(3):1145–1197, 2022.

Jared C. Carbone and V Kerry Smith. Evaluating policy interventions with general equilibrium externalities. *Journal of Public Economics*, 92(5-6):1254–1274, 2008.

S. Channan, K. Collins, and W. R. Emanuel. Global mosaics of the standard modis land cover type data. http://glcf.umd.edu/data/lc/, 2014. University of Maryland and the Pacific Northwest National Laboratory, College Park, Maryland, USA. Accessed: 2016-07-26.

Kenneth Y. Chay and Michael Greenstone. Does air quality matter? evidence from the housing market. *Journal of political Economy*, 113(2):376–424, 2005.

Shuai Chen, Paulina Oliva, and Peng Zhang. The effect of air pollution on migration: Evidence from China. *Journal of Development Economics*, 156:102833, 2022.

Yuyu Chen, Avraham Ebenstein, Michael Greenstone, and Hongbin Li. Evidence on the impact of sustained exposure to air pollution on life expectancy from China's Huai river policy. *Proceedings of the National Academy of Sciences*, 110(32):12936–12941, 2013.

Seung-Hyun Cho, Haiyan Tong, John K. McGee, Q. Todd Baldauf, Richard W.and Krantz, and M. Ian Gilmour. Comparative toxicity of size-fractionated airborne particulate matter collected at different distances from an urban highway. *Environmental health perspectives*, 117(11):1682–1689, 2009.

Center for International Earth Science Information Network CIESIN. Gridded population of the world, version 4 (gpwv4) : Population count. http://dx.doi.org/10.7927/H4F47M2C, 2016. Columbia University, NASA Socioeconomic Data and Applications Center (SEDAC), Palisades, NY. Accessed 2016-11-06.

Bruno Conte, Klaus Desmet, and Esteban Rossi-Hansberg. On the geographic implications of carbon taxes. *The Economic Journal*, 2025.

José-Luis Cruz and Esteban Rossi-Hansberg. The economic geography of global warming. *Review of Economic Studies*, 91(2):899–939, 2024.

Janet Currie and Reed Walker. What do economists have to say about the clean air act 50 years after the establishment of the environmental protection agency? *Journal of Economic Perspectives*, 33(4):3–26, 2019.

Lucas W. Davis. The effect of driving restrictions on air quality in mexico city. *Journal of Political Economy*, 116(1):38–81, 2008.

Tatyana Deryugina, Garth Heutel, Nolan H. Miller, David Molitor, and Julian Reif. The mortality and medical costs of air pollution: Evidence from changes in wind direction. *American Economic Review*, 109(12):4178–4219, 2019.

Simon Dietz. Introduction to integrated assessment modeling of climate change. In Lint Barrage and Solomon Hsiang, editors, *Handbook of the Economics of Climate Change*. Elsevier, Amsterdam, Netherlands, 2025.

Esther Duflo, Michael Greenstone, Rohini Pande, and Nicholas Ryan. Truth-telling by third-party auditors and the response of polluting firms: Experimental evidence from india. *The Quarterly Journal of Economics*, 128(4):1499–1545, 2013.

EPA. Revisions to the guideline on air quality models: Enhancements to the aermod dispersion modeling system and incorporation of approaches to address ozone and fine particulate matter, 2017.

US EPA. User's guide for the assessment system for population exposure nationwide (aspen, version 1.1) model. Technical report, United States Environmental Protection Agency, 2000.

Keith O Fuglie. Total factor productivity in the global agricultural economy: Evidence from fao data. *The shifting patterns of agricultural production and productivity worldwide*, pages 63–95, 2010.

GBD. Global burden of disease study 2021: Global burden of disease collaborative network. Technical report, Institute for Health Metrics and Evaluation, 2024.

Nicolas Gendron-Carrier, Marco Gonzalez-Navarro, Stefano Polloni, and Matthew A. Turner. Subways and urban air pollution. *American Economic Journal: Applied Economics*, 14(1):164–96, 2022.

L. Giglio and C. Justice. Mod14a1 modis/terra thermal anomalies/fire daily l3 global 1km sin grid v006. http://dx.doi.org/10.5067/MODIS/MOD14A1.006, 2015. NASA EOSDIS LP DAAC. Accessed 2016-03-31.

Douglas Gollin, David Lagakos, and Michael E Waugh. The agricultural productivity gap. *The Quarterly Journal of Economics*, 129(2):939–993, 2013.

Mikhail Golosov, John Hassler, Per Krusell, and Aleh Tsyvinski. Optimal taxes on fossil fuel in general equilibrium. *Econometrica*, 82(1):41–88, 2014.

Lawrence Goulder and Marc Hafstead. Confronting the climate challenge. In *Confronting the Climate Challenge*. Columbia University Press, 2018.

Michael Greenstone. The impacts of environmental regulations on industrial activity: Evidence from the 1970 and 1977 clean air act amendments and the census of manufactures. *Journal of political economy*, 110(6):1175–1219, 2002.

Michael Greenstone, Rohini Pande, Anant Sudarshan, and Nicholas Ryan. Can pollution markets work in developing countries? experimental evidence from india. *The Quarterly Journal of Economics*, Forthcoming, 2024.

Rema Hanna and Paulina Oliva. The effect of pollution on labor supply: Evidence from a natural experiment in mexico city. *Journal of Public Economics*, 122:68–79, 2015.

Danae Hernandez-Cortes and Kyle C Meng. Do environmental markets cause environmental injustice? evidence from californiaâĂŹs carbon market. *Journal of Public Economics*, 217:104786, 2023.

George M. Hidy et al. Remote sensing of particulate pollution from space: Have we reached the promised land? *Journal of the Air & Waste Management Association*, 59(10): 1130–1139, 2009.

Stephen P Holland, Erin T Mansur, Nicholas Z. Muller, and Andrew J Yates. Are there environmental benefits from driving electric vehicles? the importance of local factors. *American Economic Review*, 106(12):3700–3729, 2016.

Alex Hollingsworth, Taylor Jaworski, Carl Kitchens, and Ivan Rudik. Economic geography and air pollution regulation in the united states. *Journal of Political Economy - Microeconomics*, Forthcoming, 2024.

IEA. Value of fossil-fuel subsidies by fuel in the top 25 countries. Technical report, International Energy Agency, 2023. URL `https://www.iea.org/data-and-statistics/charts/value-of-fossil-fuel-subsidies-by-fuel-in-the-top-25-countries-2022`.

IEA. Iea energy prices. Technical report, International Energy Agency, 2024. URL `https://www.iea.org/data-and-statistics/data-product/energy-prices`.

Koichiro Ito and Shuang Zhang. Willingness to pay for clean air: Evidence from air purifier markets in China. *Journal of Political Economy*, Forthcoming, 2019.

B. Kelsey Jack, Seema Jayachandran, Namrata Kala, and Rohini Pande. Money (not) to burn: payments for ecosystem services to reduce crop residue burning. *American Economic Review: Insights*, Forthcoming, 2024.

B Kelsey Jack, Seema Jayachandran, Namrata Kala, and Rohini Pande. Money (not) to burn: payments for ecosystem services to reduce crop residue burning. *American Economic Review: Insights*, 7(1):39–55, 2025.

Daniel Jacob. *Introduction to atmospheric chemistry*. Princeton University Press, 1999a.

Daniel Jacob. *Introduction to atmospheric chemistry*. Princeton University Press, 1999b.

P. D. Jones and I. C. Harris. Cru ts3.10: Climatic research unit (cru) time-series (ts) version 3.10 of high resolution gridded data of month-by-month variation in climate (jan. 1901 - dec. 2014), 2013. NCAS British Atmospheric Data Centre. Accessed 2017-6-17.

Mikael Karlsson, Eva Alfredsson, and Nils Westling. Climate policy co-benefits: a review.

Climate Policy, 20(3):292–316, 2020.

Gaurav Khanna, Wenquan Liang, Ahmed Mushfiq Mobarak, and Ran Song. The productivity consequences of pollution-induced migration in China. *American Economic Journal: Applied Economics*, Forthcoming, 2024.

Khaled H Kheiravar and C-YC Lin Lawell. The effects of fuel subsidies on air quality: Evidence from the iranian subsidy reform. Technical report, Working paper, Cornell University, 2020.

Christopher R Knittel, Douglas L Miller, and Nicholas J Sanders. Caution, drivers! children present: Traffic, pollution, and infant health. *Review of Economics and Statistics*, 98(2):350–366, 2016.

Rob Levy, Christina Hsu, and al. Modis atmosphere l2 aerosol product b. http://dx.doi.org/10.5067/MODIS/MOD04_L2.006, 2015. NASA MODIS Adaptive Processing System, Goddard Space Flight Center, USA. Accessed: 2015-09-24.

Gilbert E. Metcalf. *Paying for pollution: why a carbon tax is good for America*. 2018.

Melanie Morten and Jaqueline Oliveira. The effects of roads on trade and migration: Evidence from a planned capital city. *NBER Working Paper*, 22158:1–64, 2018.

Nicholas Z. Muller and Robert Mendelsohn. Measuring the damages of air pollution in the united states. *Journal of Environmental Economics and Management*, 54(1):1–14, 2007.

Nicholas Z. Muller and Robert Mendelsohn. Efficient pollution regulation: getting the prices right. *American Economic Review*, 99(5):1714–39, 2009.

William D Nordhaus. *A question of balance: Weighing the options on global warming policies*. Yale University Press, 2008.

William D Nordhaus. Revisiting the social cost of carbon. *Proceedings of the National Academy of Sciences*, 114(7):1518–1523, 2017.

Lindsey Norgrove and Stefan Hauser. Estimating the consequences of fire exclusion for food crop production, soil fertility, and fallow recovery in shifting cultivation landscapes in the humid tropics. *Environmental management*, 55(3):536–549, 2015.

OECD. *Taxing Energy Use 2019: Using Taxes for Climate Action*. OECD Publishing, Paris, 2019. URL `https://doi.org/10.1787/058ca239-en`.

OECD/IEA. World energy statistics. IEA Publishing, 2018.

Paulina Oliva. Environmental regulations and corruption: Automobile emissions in mexico city. *Journal of Political Economy*, 123(3):686–724, 2015.

Chris Papageorgiou, Marianne Saam, and Patrick Schulte. Substitution between clean and dirty energy inputs: A macroeconomic perspective. *Review of Economics and Statistics*, 99(2):281–290, 2017.

Ian WH Parry, Mr Dirk Heine, Eliza Lis, and Shanjun Li. *Getting energy prices right: From principle to practice*. International Monetary Fund, 2014.

Lara Aleluia Reis, Laurent Drouet, and Massimo Tavoni. Internalising health-economic impacts of air pollution into climate policy: a global modelling study. *The Lancet Planetary Health*, 6(1):e40–e48, 2022.

Dede Rohadi. Zero-burning policy hurts small farmers âĂŞ a flexible approach is needed. *The Conversation*, September 12, 2017.

HS Sidhu, Manpreet Singh, Yadvinder Singh, John Blackwell, Shiv Kumar Lohan, Elizabeth Humphreys, ML Jat, Vicky Singh, and Sarbjeet Singh. Development and evaluation of the turbo happy seeder for sowing wheat into heavy rice residues in

NW india. *Field Crops Research*, 184:201–212, 2015.

Jason D. Tessum, Christopher W.and Hill and Julian D Marshall. Inmap: A model for air pollution interventions. *PloS one*, 12(4):e0176131, 2017.

Peter Tschofen, Inês L. Azevedo, and Nicholas Z. Muller. Fine particulate matter damages and value added in the US economy. *Proceedings of the National Academy of Sciences*, 116(40):19857–19862, 2019.

Aaron Van Donkelaar, Randall V Martin, Michael Brauer, N Christina Hsu, Ralph A Kahn, Robert C Levy, Alexei Lyapustin, Andrew M Sayer, and David M Winker. Global estimates of fine particulate matter using a combined geophysical-statistical method with information from satellites, models, and monitors. *Environmental science & technology*, 50(7):3762–3772, 2016.

Atheendar S Venkataramani and Brian J Fried. Effect of worldwide oil price fluctuations on biomass fuel use and child respiratory health: evidence from guatemala. *American journal of public health*, 101(9):1668–1674, 2011.

W.Kip Viscusi and Joseph E. Aldy. The value of a statistical life: a critical review of market estimates throughout the world. *Journal of risk and uncertainty*, 27(1):5–76, 2003.

W. Reed Walker. The transitional costs of sectoral reallocation: Evidence from the clean air act and the workforce. *The Quarterly journal of economics*, 128(4):1787–1835, 2013.

WB. Beyond mitigation: Quantifying the development benefits of carbon pricing. Technical report, World Bank, Washington, DC, 2021. URL `https://hdl.handle.net/10986/35624`.

Jeff Wen, Sam Heft-Neal, Patrick Baylis, Judson Boomhower, and Marshall Burke. Quantifying fire-specific smoke exposure and health impacts. *Proceedings of the National Academy of Sciences*, 120(51):e2309325120, 2023.

F.J. Wentz, J. Scott, R. Hoffman, M. Leidner, R. Atlas, and J. Ardizzone. Remote sensing systems cross-calibrated multi-platform (ccmp) 6-hourly ocean vector wind analysis product on 0.25 deg grid, version 2.0, january 2000 to december 2015. www.remss.com/measurements/ccmp, 2015. Remote Sensing Systems, Santa Rosa, CA. Accessed 2017-6-27.

World Bank. Urban population (% of total), world development indicators. https://datacatalog.worldbank.org/dataset/world-development-indicators, 2018.

Yanan Wu, Jiakai Liu, Jiexiu Zhai, Ling Cong, Yu Wang, Wenmei Ma, Zhenming Zhang, and Chunyi Li. Comparison of dry and wet deposition of particulate matter in near-surface waters during summer. *PloS one*, 13(6):e0199241, 2018.

Appendix A. Calibration

The calibration proceeds in three steps. First, we set certain parameters based on the literature or standard assumptions at common values for all countries (“Directly Calibrated”). Second, we back out certain parameter values directly from data for each country (“Directly based on Data”). Third, we select the remaining model parameters

Table A1: Directly calibrated parameters

Parameter	Value(s)	Sources and Notes
α	0.33	Standard
ρ_L^{Ag}	0.52	Combine Fuglie (2010) cross-country estimates,
ρ_K^{Ag}, ρ_J^{Ag}	0.32, 0.05	Gollin, Lagakos, and Waugh (2013), and modeler's judgment
ε	2	GHKT (2014)
σ	1.5	Nordhaus (2008)
R^*	0.15	Real return of 5%/year plus 10% depreciation
ρ	$100\frac{\mu g}{m^3}$	Gendron-Carrier et al. (2022)

Table A2: Fuglie (2010): Agricultural factor share estimates (Weighted Global Avg.)

Labor	Land & Structures	Livestock & Feed	Machinery & Energy	Chemicals & Seed
0.35	0.21	0.23	0.10	0.10

to jointly minimize the sum of squared differences between equilibrium moments as observed in the data and our model ("Matching Moments").

Directly Calibrated

Table A1 summarizes the parameters calibrated based on the literature. The agricultural production parameters warrant further discussion. Fuglie (2010) reviews empirical estimates of agricultural input elasticities across countries and computes weighted global averages over the categories given in table A2. Based on these figures, we assign "Land & Structures" equally between land and capital, split "Machinery & Energy" equally between capital and energy, and attribute the remaining materials inputs proportionally to labor and capital. Reassuringly, the resulting labor share estimate of $\rho_L^{Ag} = 0.52$ matches Gollin, Lagakos, and Waugh's (2013) insight that empirical evidence on agriultural cost shares from share tenancy arrangements suggest that 50-50 splits between labor and other factors are common across countries and time.

The burning abatement cost function parameters are more challenging to calibrate. Select estimates exist. For example, Norgrove and Hauser (2015) find that "fire exclusion led to an approximately 50% increase in labor requirements for planting, weeding, and harvesting both in the maize and plantain systems" in the Congo Basin. In surveys, Indonesian farmers have reported that clearing peatland manually requires one to two months time for what could be accomplished by fire in a few days (Rohadi (2017)). In India, it is commonly reported that the labor cost for manual harvesting - which avoids the stubble that otherwise needs to be burned - is currently around Rs 3,000 - 4,000 per acre, whereas the cost of renting a combine machine (which does not clear the stubble) is Rs 1,500-2,000, suggesting a doubling of harvesting costs for full fire abatement. We proceed as follows. First, we assume a standard convexity parameter of ν_2=2. The parameter $\nu_{1,m}$ captures the fraction of each country m's agricultural output that it would cost to fully eliminate burning (as $\Omega_m(\mu_m = 1)$=$\nu_{1,m}$). For burning crops, we take as central estimate that eliminating residue burning increases labor costs by 40 percent for relevant crops. Since not all crops are associated with burnable residue, we scale the overall cost estimate by each country's relative importance of burning crops. More formally, letting $\omega_{B,m}$ denote the share of burning crops in m, the fraction of output required to eliminate agricultural burning emissions is thus given by:

$$\Omega_m(\mu_m = 1) = 1 - [(1 - \omega_{B,m}) + \omega_{B,m}(1 - 0.4)]^{\rho_L^M} \tag{A1}$$

We quantify $\omega_{B,m}$ as follows. First, we use Food and Agriculture Organization data to compute the share of land devoted to burning crops in each country (in 2010), where we classify as "burning" all crops listed in FAOSTAT data for crop residue burning (rice, sugar cane, wheat, and maize). The largest burning shares observed are around 80 percent. Second, we compute each country's residue burning intensity in MT/$ based on our data (from IIASA and the World Bank, respectively). The highest agricultural burning intensity country in 2010 was South Africa. We then set $\omega_{B,m}$=0.80 for South Africa, and decrease $\omega_{B,m}$ proportional to each country's relative agricultural burning intensity differential (i.e., the percentage deviation relative to the maximum).

Directly based on Data:

We now describe the parameters and initial equilibrium values based directly on data.

Economic Model: Base year fuel input usage across sectors ($E^j_{c,m}$, $E^j_{p,m}$, $E^j_{g,m}$ for $j \in I; S, Ag$) are from the International Energy Agency (OECD/IEA (2018)). We map the data into model sectors as follows: "Agriculture" contains IEA sectors Agriculture and Forestry, and Fishing. "Services" contains IEA sectors Residential, Commercial and public services, and Transport. Finally, "Industry" contains IEA sector Industry.

Energy resource prices are from British Petroleum Company (2016). We average across global prices for each fuel to compute p^*_c, p^*_p, and p^*_g (calibrated based on natural gas prices) and then adjust by the energy content of the fuel to arrive at prices per Mtoe.

Based on these prices and quantities, we can then directly back out each sector's energy production κ's for each country from the energy service producers' optimality conditions (standard, see Online Appendix equations (OA4)-(OA5)) and the assumption that $1 = \kappa^j_{c,m} + \kappa^j_{p,m} + \kappa^j_{g,m}$ for each $j \in I,S,Ag$.

With values for fuel inputs and energy production parameters in hand, we can infer each sector's energy aggregate production $J^I_m \equiv J^{I,u}_m + J^{I,a}_m$, J^S_m, and J^{Ag}_m in the country-year via equations (2, 4, 8). We can then infer each country's base year aggregate energy input prices for each sector $p^I_{J,m}$, $p^S_{J,m}$, and $p^{Ag}_{J,m}$ from the relevant fuel price indexes

$$p^j_{J,m} = \left((\kappa^j_{c,m})^{\varepsilon} (p^*_c + \tau^j_{c,m})^{1-\epsilon} + (\kappa^j_{p,m})^{\varepsilon} (p^*_p + \tau^j_{p,m})^{1-\epsilon} + (\kappa^j_{g,m})^{\varepsilon} (p^*_g + \tau^j_{g,m})^{1-\epsilon} \right)^{\frac{1}{1-\varepsilon}},$$

for $j \in \{I,a; I,u; S,Ag\}$. As a benchmark we set pre-existing taxes to zero for individual fuels. However, we allow for and back out from the data a rural industry energy wedge τ^{Ja}_m as described in the "Matching Moments" section below.

For each country, we then set energy expenditure shares (ν^I_m, ν^S_m, $\rho^{Ag}_{J,m}$) based on the observed base year share. For example (and analogously for other sectors):

$$\nu^I_m = \frac{p^I_{J,m} \cdot J^I_m}{Y^I_m}$$

The emissions coefficients for each fuel type (ξ^c_m, ξ^p_m, ξ^g_m) are based on IIASA GAINS model data described in Section 6. The specifics are as follows. First, we obtain IIASA's estimates of each country's total PM10 *emissions* by fuel/activity for all available years of our sample (2000, 2005, 2010, 2015).[20] Second, we obtain IIASA's estimates of each country's energy use by key fuel type (coal, liquid fuel, natural gas, etc.). Finally, we divide emission from each fuel by fuel quantity to derive *emissions coefficients* (KT of PM10 per PJ) for each fuel type-country-year.[21]

The emissions coefficient for industrial output (ξ^I_m) is derived by dividing non-combustion industrial emissions totals for each country-year (from IIASA) by industry output in the relevant country-year. The emissions coefficient for services (ξ^S_m) is also derived by dividing IIASA's estimates of total non-exhaust road emissions by services output in the relevant country-year. The emissions coefficient for agricultural *output* combines IIASA's estimates of (i) non-burning related agricultural emissions (e.g., fertilizer use) and (ii) emissions from general biomass energy inputs. The sum of these terms is then divided by agricultural output in the relevant country-year.

[20] We specifically consider the ECLIPSE_v5a_CLE_base scenario which reflects current law.

[21] We note that IIASA also makes publicly available the extremely detailed activity data and fuel coefficient estimates underlying their analysis. These differentiate, for example, coal emissions coefficients of pulverized versus fluidized bed versus grate firing combustion boilers. IIASA's total emissions data reflect their estimates of the distribution of these technologies within each country-year. Our use of these total emissions along with energy inputs data thus yields an appropriately weighted average emissions factor at the fuel level, as relevant for our analysis.

The emissions coefficient for agricultural burning (ξ_m^B) is obtained directly from IIASA's estimates ("Emissions factors and related parameters for PM (TSP) and CO2"), specifically as the PM10 emissions coefficient for the "WASTE_AGR" variable.

For household preference parameters, we consult World Bank data on sectoral household expenditures across countries from 2010. First, we map the reported categories into our model's basic sectors according to the following correspondence: "Industry" contains World Bank sectors Clothing and Footwear, Energy, ICT , and Others. "Services" contains World Bank sectors Education, Financial Services, Health, Housing, Personal Care,Transport, and Water Utility. Finally, "Agriculture" is the World Bank Food and Beverages sector. Second, because the data do not cover all of our sample countries, we extrapolate consumption shares for countries with missing data. Letting $D_{j,2010}^{Inc}$ denote the GDP per capita quintile of country j in 2010, we estimate

$$\theta^{I,j,2010} = \beta_0 + \sum_{j=1}^{4} \beta_j D_{j,2010}^{Inc} + \varepsilon_j$$

and use predicted shares $\widehat{\theta^{I,j}}$ where needed. Third, given that the model treats the services sector as non-traded, in order to better match its output data, we set the service sector consumption share based on observed base year service sector *output* shares:

$$\theta_m^S = \tilde{Y_m^S} / Y_m$$

where $\tilde{Y_m^S}$ denotes service sector GDP and Y_m total GDP. Finally, the remaining good (here agriculture) expenditures share is then set as the residual based on:

$$1 = \theta_m^I + \theta_m^S + \theta_m^{Ag}$$

Finally, based on the structure of the model, we can back out initial equilibrium levels of capital in both services and agriculture:

$$K_m^S = \alpha \cdot \widetilde{Y_m^S} / R^*$$
$$K_m^{Ag} = \rho_K^{Ag} \cdot \widetilde{Y_m^{Ag}} / R^*$$

where the tilde marks output *values* (i.e., $p \cdot Y$) as observed in sectoral GDP data.

Particulates model:

Dry deposition velocities are based on the EPA's ASPEN model (EPA (2000)). Their analysis presents different deposition velocity values depending on (i) urban versus rural areas, (ii) wind speed, and (iii) atmospheric stability. We adopt values relevant to each region (urban or rural), compute weighted (based on border lengths) average wind speeds for each area, and assume neutral atmospheric stability to select the appropriate deposition velocity for a given country-region. ASPEN provides dry deposition rates. We adjust for the average prevalence of wet deposition through a proportional increase of +37% based on estimates by Wu et al., (2018).[22]

Mixing height λ is set to 0.5 km based on data from the EPA's Support Center for Regulatory Atmospheric Modeling (SCRAM). SCRAM previously provided twice daily mixing height observations across the United States at the monitoring station level. The data contain at least one station per state, including coverage in Hawaii and Alaska, thus reflecting a very diverse set of climatic and geographic areas. In the most recent year of observations (1991), the average morning mixing high recorded is 487 meters.

Matching Moments

Given the data and calibrated values described thus far, we select the remaining unknown parameters and initial equilibrium values to minimize the squared sum of differences between the model's equilibrium conditions and the data: Sectoral productivities $A_m^{I,u}$, $A_m^{I,a}$, A_m^S A_m^{Ag}; industry allocations across urban and rural areas $K_m^{I,u}$, $K_m^{I,a}$, $L_m^{I,u}$, $L_m^{I,a}$, $J_m^{I,u}$, $J_m^{I,a}$, $Y_m^{I,u}$, $Y_m^{I,a}$; labor allocations towards the other sectors L_m^{Ag}, L_m^S; prices p_m^S, p^{Ag^*}, w_m^u, w_m^a; household consumption bundles c_m^I, c_m^S, c_m^{Ag}, x_m^I, x_m^S, x_m^{Ag}; and a rural industry energy services tax wedge $\tau_{J,m}^{I,a}$. Initial experimentation suggested that equal marginal products of energy services between rural and urban industry is difficult to match. We therefore allow for a rural energy services tax wedge defined by:

$$\frac{v_m^I Y_m^{I,a}}{J_m^{I,a}} = p_{J,m}^a(1+\tau_{J,m}^{I,a}) \tag{A2}$$

Another point to note is that our model assumes that households earn only labor income and that returns to capital are paid abroad. Consequently, the model under-estimates household income levels relative to reality. In order to match the model's implied household demand for services to an empirical moment, we thus use observed services output adjusted by the approximate labor income fraction, specifically:

$$((L_m^{I,a}+L_m^{Ag})x_m^S + (L_m^{I,u}+L_m^S)c_m^S)p_m^S = \tilde{Y_m^S}(1-\alpha-max(\nu_m^I,\nu_m^S,\rho_{J,m}^{Ag}))$$

The remainder of the calibration proceeds as follows. Given industry energy demands ($J_m^{I,u}$, $J_m^{I,a}$) we can then back out the implied fuel usages in each area ($E_{c,m}^{I,u}$, $E_{c,m}^{I,u}$, $E_{c,m}^{I,u}$,

[22]In countries where the exogenous emissions ($Emiss_{EX}^s$ or $Emiss_{EX}^r$) implied by the benchmark calibration at baseline AOD and emissions levels are negative, we further adjust the deposition rates to the minimum level required to ensure that exogenous emissions are non-negative.

$E^{I,u}_{c,m}$, $E^{I,u}_{c,m}$, $E^{I,u}_{c,m}$). Given each country's preference parameters and domestic price levels, we then also set the particulates disutility parameters to match the model's implied marginal willingness to pay (MWTP) to empirical estimates:

$$MWTP^{AOD}_m = \frac{-MU^{AOD}_m}{MU_{c_{I,m}}} = \frac{\chi_{1,m}(\chi_2)(AOD^u_m)^{\chi_2-1}}{\widetilde{c_m}^{1-\sigma}\theta^I_m(c^I_m)^{-1}}$$

We set $\chi_2 = 2$ and select $\chi_{1,m}$ so that $MWTP_{AOD}$ equals 1.16 - Ito and Zhang's (2019) 5-year estimate of $5.46 per household annualized at a 3% annual discount rate - when evaluated at the relevant income ($2,253.5) and AOD of 1.15 (PM10 levels of 115 $\frac{\mu g}{m^3}$).

Finally, omitting country subscripts briefly for legibility, we calibrate the rural amenity GEV distributions parameters as follows. The GEV distribution in each country depends on a shape parameter shp, a location parameter loc, and a scale parameter scl, with associated pdf for $shp \neq 0$:

$$f(x) = (\frac{1}{scl})exp(-(1+shp(\frac{(x-loc)}{scl}))^{-\frac{1}{shp}})(1+shp(\frac{(x-loc)}{scl}))^{-1-\frac{1}{shp}}$$

for $(1+shp(\frac{(x-loc)}{scl})) > 0$ and, for $shp = 0$,

$$f(x) = (\frac{1}{scl})exp(-exp(-\frac{(x-loc)}{scl}) - \frac{(x-loc)}{scl}).$$

We calibrate shp, loc and scl from three moments: First, after calculating the initial equilibriu, marginal rural amenity value ε^* via (17), we ensure that the GEV distribution matches the initial observed urban population share u^*_0 in each country via:

$$u^*_0 = F(\varepsilon^*)$$

where $F(.)$ denotes the CDF of the GEV distribution in a given country. Second, we match the assumed migration-wage elasticity ϵ_{mig-w} = 1.9 based on Morten and Oliveira (2018) by calculating counterfactual values of the urban population share $\tilde{u_0}$ and marginal rural amenity value $\tilde{\varepsilon}$ after a hypothetical 1% urban wage increase and ensuring that these are consistent with the GEV distribution via:[23]

$$\tilde{u_0} = F(\tilde{\varepsilon})$$

Third, we select the location parameter loc to fit the standard GEV property:

$$F(loc) = exp(-1)$$

For each country, our calibration searches for values of the scale, shape, and location parameters of a GEV distribution to match these three moments as closely as possible.

[23]The counterfactual values are $\tilde{u_0} = min\{1, u^*_0 \cdot (1+\epsilon_{mig-w})\}$ and $\tilde{\varepsilon}$ from (17) with urban consumption $\tilde{c}$ re-calculated at a 10% higher wage (in partial equilibrium without changes in AOD or output prices).

Online Appendix for:

Equilibrium Particulate Exposure

Lorenzo Aldeco, Lint Barrage, and Matthew Turner

March 2026

OA1. Additional Figures and Tables

Figure OA1: World maps of AOD and population in 2010

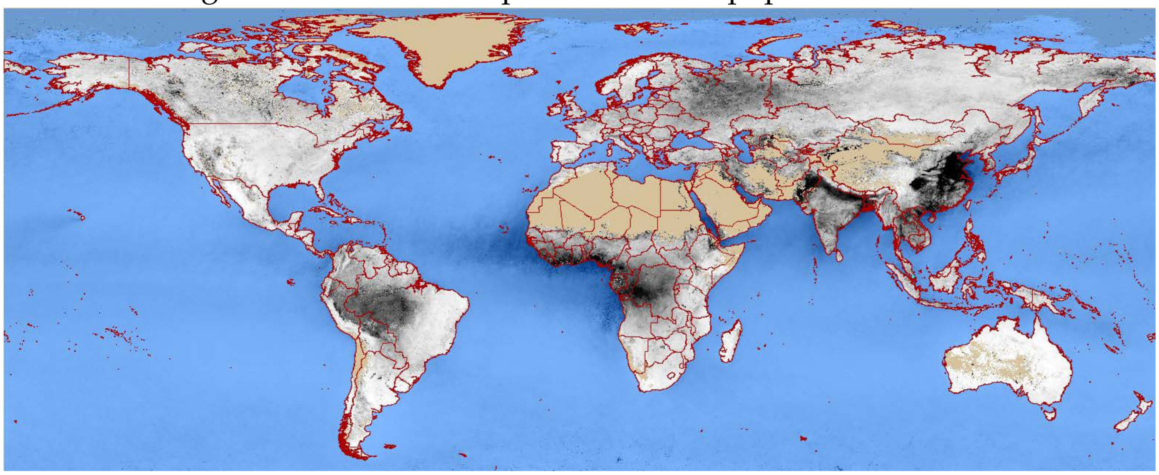

(a) Aerosol Optical Depth, 2010

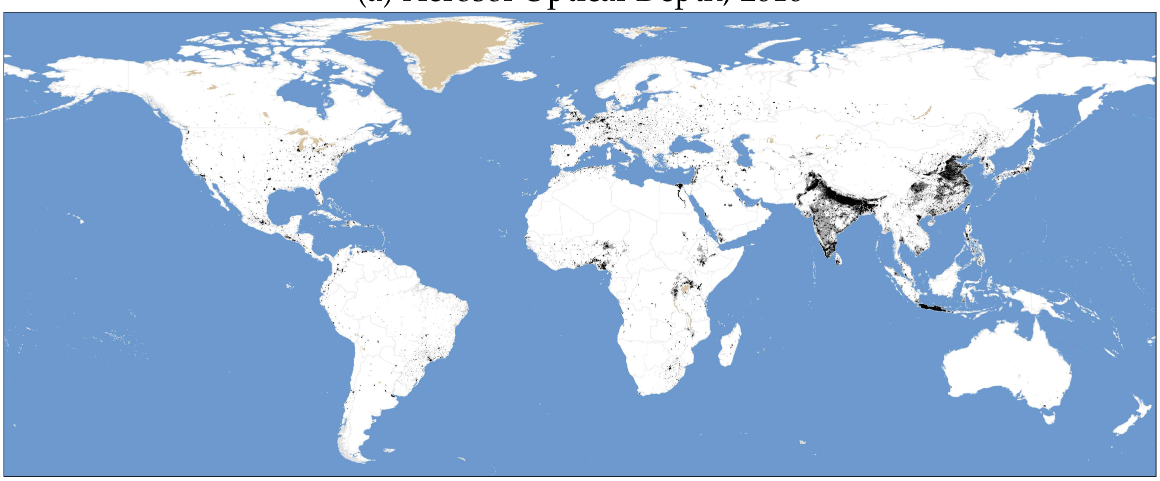

(b) Gridded Population of the World, 2010

Note: *(a) Shows annual average aerosol optical depth as measured by MODIS for 2010 (Levy et al., 2015). (b) shows population density in 2010 as reported by CIESIN (2016). In both figures, darker colors indicate higher values and tan indicates missing data.*

Table 4 shows that country level variation can explain close to half of all variation in exposure. We now investigate the extent to which additional pixel level variation is important for exposure. Table OA1 repeats variants of the population weighted regression of column 6 of table 4 where we add pixel-year level covariates. Sample sizes in table OA1 are smaller than in table 4 because of missing values for pixel level variables.

Column 1 estimates the effect of pixel-year population density on exposure. Unsurprisingly, people who live in denser places experience higher particulate exposure. In-

Figure OA2: Fuel consumption, urban boundaries and cross-border flows in 2010

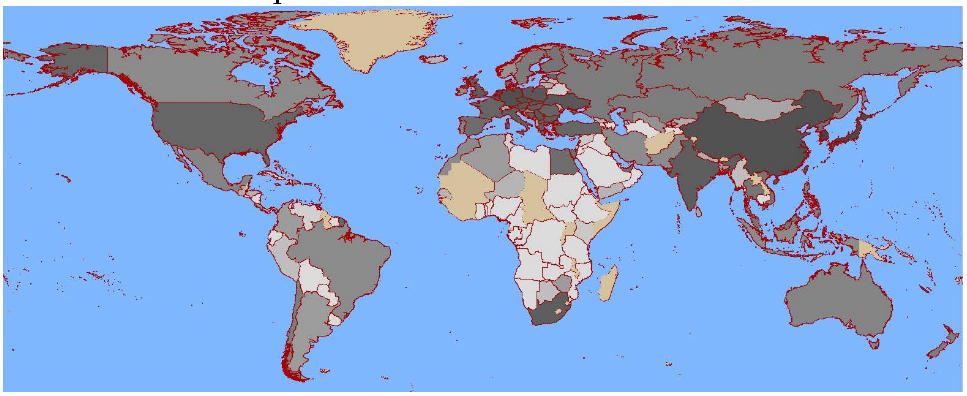

(a) Coal consumption, annual Mtoe per km^2

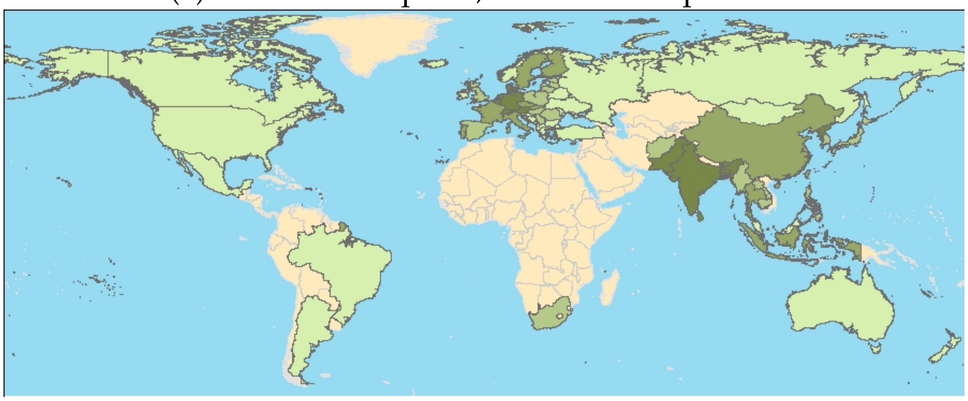

(b) Organic fuel consumption, annual PJ per km^3

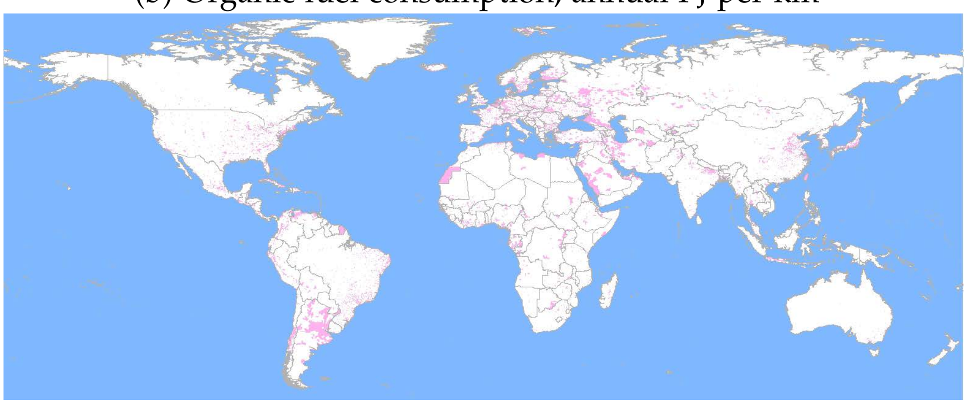

(c) Urban and rural regions, 2010

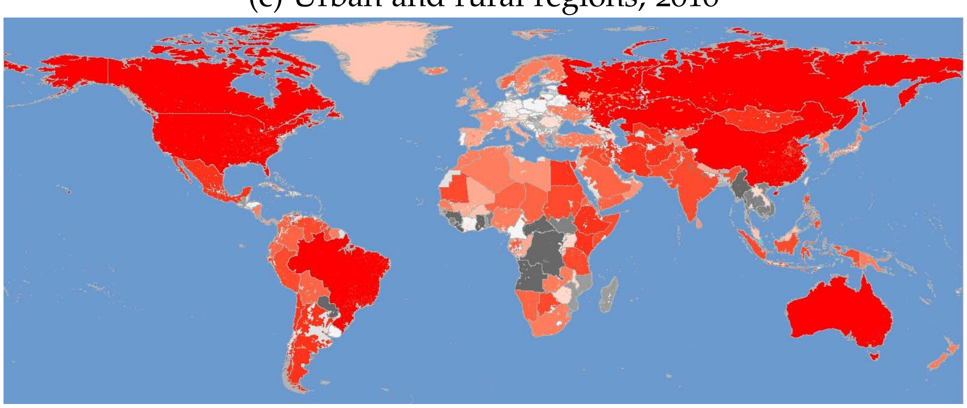

(d) Net Flows, annual κτ per km^3

creasing the population of a 10km^2 pixel by 100,000 people increases expected exposure by about 0.7 AOD points. Converting to PM10, this is about 70 μg/m^2, the difference between a clean coastal city in the developed world and a large Chinese city. While this response seems large, it improves our ability to predict exposure only slightly. The R^2 in this regression is only marginally higher than column 6 of table 4, 0.57 vs 0.56.

The second column of table 4 includes our pixel level urban indicator (illustrated in figure OA2(c)) instead of density. On average people living in urban pixels are exposed to about 0.1 extra AOD points, about 10μg/m^2 PM10. This indicator variable is also highly significant, but like population density, does little to improve our ability to predict exposure. The indicator variable reduces our prediction error by slightly more than does the linear term in density, so the step function in density implied by the indicator variable is a better predictor of AOD than the linear function of column one. The geography of our model is partly motivated by this finding. In our model, each country is divided into rural and urban regions.

Columns 3 and 4 include remotely-sensed measures of land cover, share in crops and share barren. Both are sources of dust, and unsurprisingly, contribute to exposure. These results indicate that exposure is not purely anthropogenic, physical geography plays a role. Finally, column 5 includes our remotely-sensed measure of fire intensity in the pixel. This coefficient is not measurably different from zero. This reflects the physical geography of smoke dispersion. The smoke plumes from wildfires often spread out over much larger areas than one of our 10km^2 pixels (Wen et al., (2023)).

Table OA1 column 6 replicates the regression of table 4 column 6, but includes all five of our pixel year level variables. The R^2 of this regression is only 0.63, versus about 0.56 for the regression including only country-year indicators and climate variables. That is, high quality, spatially disaggregated measures of particulate sources barely improves our ability to predict exposure once we know country-year of residence.

We next investigate the extent to which country-year level variation in exposure can be attributed to country-year level variation in economic fundamentals. In table OA2, we present pixel level regressions of AOD on variables that vary only at the level of the country-year. These regressions are population weighted, and so measure the ability of particular country-year level variables to predict exposure.

Columns 1-3 include measures of natural gas and renewables, coal, and petroleum per square kilometer of country area one by one. Holding mixing height constant these variables are proportional to consumption per unit of country mixing volume. Because the physical process that determines concentration depends on contributions to particulate mass per unit volume, not country level particulate mass, these normalized variables are more relevant to an investigation of concentration and exposure than are country level aggregates.

That the sign on green is negative points to an inference problem that helps to motivate our model. While natural gas, wind, and solar power cause essentially zero particulate emissions, all else equal, they do not reduce concentration. More likely, countries that rely more heavily on these fuels also rely less heavily on dirtier power sources. This regression describes an equilibrium relationship, not a causal one.

Column 2 estimates the relationship between coal and exposure. We see that country-year level coal consumption has an R^2 of 0.14. In column 3, we see that country-year level oil consumption is positively related to equilibrium exposure, but like clean power, it has little predictive ability.

Columns 4 and 5 look at the effect of organic fuel consumption and agricultural burning per square km. These variables have the expected positive signs and even more ability to predict exposure than coal consumption.

Column 6 of table OA2 estimates the effect of the share of a country's area that is urban on particulate exposure. Consistent with what we see in figure 1, urbanization predicts exposure and this variable has an R^2 higher than that of coal. However, the sign on this variable is negative, contrary to what we saw in table OA1. Taken together, the results table OA1 and OA2 suggest the importance of urbanization as a determinant of equilibrium levels of exposure, but also indicate the importance of a model or quasi-random variation if we are to estimate a causal relationship.

Columns 7-9 examine the role of GDP in services, industry and agriculture, also per unit of area, on exposure. Production in services has little ability to predict exposure. Countries that produce more agricultural and industrial products have greater particulate exposure, although only agricultural GDP has much ability to predict exposure.

Column 10 estimates the effect of mass per square kilometer of cross-border flows in an out of each country. As expected, flows in increase exposure and conversely for flows out. These two variables have an R^2 of 0.04.

Column 11 conducts a regression including all of these country-year level regressors. Two findings are noteworthy. First is the relative stability of coefficient estimates. With the exception of natural gas and green power generation, none of the coefficients change signs relative to the regression where the relevant regressor appears alone. Second, the R^2 of this regression is 0.39. In contrast, the R^2 in column 3 of table 4 (the comparable specification) is 0.46. That is, this relatively short list of likely suspects explains most of the variation in exposure that can be explained by factors that vary at the country-year level. Therefore, these results also indicate the importance of national particulates policy.

Table OA1: Population weighted regressions of AOD on pixel-year level sources, country-year indicators and climate. 30 country calibration sample, 2000, 2005, 2010, 2015.

	(1)	(2)	(3)	(4)	(5)	(6)
Density	0.00000756***					0.00000814***
	(0.000000457)					(0.000000834)
Urban		0.101***				0.0823***
		(0.00133)				(0.00234)
Crops			0.000255***			0.000402***
			(0.00000711)			(0.00000746)
Barren				0.00130***		0.00182***
				(0.0000757)		(0.000119)
Fire					0.000106	0.00000439
					(0.000118)	(0.000115)
N	3635382	3636452	3636452	3636452	3636452	3635382
R^2	0.573	0.592	0.574	0.562	0.559	0.629

Note: *Robust standard errors in parentheses. Controls for country-year fixed effects in all specifications.* * $p < 0.05$, ** $p < 0.01$, *** $p < 0.001$

Finally, comparing table OA2 to table 2 we see that the regressions results are broadly consistent with raw data describing emissions, although the raw emissions data suggests a relatively larger role for coal than do the regressions.

OA2. Competitive Equilibrium Details

This section elaborates details of the competitive equilibrium not already in Section 5. We here omit country subscripts for legibility.

Production: First, sectoral outputs $\{Y^{I,u}, Y^{I,a}, Y^{S}, Y^{M}, J^{I,u}, J^{I,a}, J^{S}, J^{M}\}$ are produced acccording to the production technologies (1)-(8). Second, profit-maximizing input demands equate marginal products to factor prices for each type of producer. For industry and services, these conditions are given by:

$$\frac{(1-\alpha-v^m)Y^m}{L^m} = w^k \tag{OA1}$$

$$\frac{\alpha Y^m}{K^m} = R^* \tag{OA2}$$

$$\frac{v^m Y^m}{J^m} = p^{J,m} \tag{OA3}$$

$$m \in \{I,u; I,a; S\} \text{ and } k = \begin{cases} u & \text{if } m \in \{I,u; s\} \\ a & \text{if } m \in \{I,a\} \end{cases}$$

Table OA2: Population weighted regressions of AOD on country-year level sources, *without* country-year indicators or climate. 30 country calibration sample, 2000, 2005, 2010, 2015.

	(1)	(2)	(3)	(4)	(5)	(6)	(7)	(8)	(9)	(10)	(11)
	Terra	Terra	Terra	Terra	Terra	Terra	Terra	Terra	Terra	Terra	Terra
Green/km^3	-33										248
	(163)										(167)
Coal/km^3		347***									264**
		(70)									(99)
Oil/km^3			-6								-270***
			(21)								(59)
Ag burn/km^3				2792***							29
				(577)							(520)
Biomass/km^3					59***						8.5
					(9.6)						(14)
Urb. share						-.0057***					-.0019
						(.0011)					(.0012)
Srv GDP/km^3							-.0016				-.033**
							(.0056)				(.0098)
Ind GDP/km^3								.051*			.095*
								(.023)			(.037)
Ag GDP/km^3									.51***		.21**
									(.072)		(.071)
Flow-/km^3										-152**	76
										(55)	(71)
Flow+/km^3										161**	-38
										(57)	(64)
N	3640600	3640600	3640600	3640600	3640600	3640600	3640600	3640600	3640600	3640600	3640600
R^2	0.000	0.135	0.000	0.150	0.165	0.170	0.000	0.051	0.237	0.036	0.389

Note: *Standard errors in parentheses clustered at the country-year level.* * $p < 0.05$, ** $p < 0.01$, *** $p < 0.001$

For energy producers, the corresponding fuel input demands are:

$$\frac{E_c^m}{E_p^m} = \left(\frac{\kappa_c^m}{\kappa_p^m}\left(\frac{p_p^* + \tau_p^m}{p_c^* + \tau_c^m}\right)\right)^{\varepsilon} \quad \text{(OA4)}$$

$$\frac{E_c^m}{E_g^m} = \left(\frac{\kappa_c^m}{\kappa_g^m}\left(\frac{p_g^* + \tau_g^m}{p_c^* + \tau_c^m}\right)\right)^{\varepsilon} \quad \text{(OA5)}$$

$$m \in \{I,u; I,a; S,M\}$$

Finally, in agriculture, the profit-maximizing conditions for input demands and waste burning B are given by:

$$\rho_L^M \frac{Y^M}{L^M}\left[p^{M^*} - \tau_B(1-\mu)\xi^B\right] = w^a \quad \text{(OA6)}$$

$$\rho_K^M \frac{Y^M}{K^M}\left[p^{M^*} - \tau_B(1-\mu)\xi^B\right] = R^* \tag{OA7}$$

$$\rho_J^M \frac{Y^M}{J^M}\left[p^{M^*} - \tau_B(1-\mu)\xi^B\right] = p_J^M \tag{OA8}$$

$$\nu_1\nu_2\mu^{\nu_2-1}\left[p^{M^*} - \tau_B(1-\mu)\xi^B\right] = \xi^B\tau_B(1-\nu_1\mu^{\nu_2}) \tag{OA9}$$

$$\tag{OA10}$$

Households: The optimal consumption bundle for urban households maximizing their utility (13) subject to budget constraint (15) satisfy optimality conditions:

$$\frac{(1-\theta^I-\theta^S)}{\theta^I}\frac{c^I}{c^M} = p^{M^*} \tag{OA11}$$

$$\frac{\theta^S}{\theta^I}\frac{c^I}{c^S} = p^S \tag{OA12}$$

Analogously, for rural households, consumption bundles satisfy the budget constraint (16) and:

$$\frac{(1-\theta^I-\theta^S)}{\theta^I}\frac{x^I}{x^M} = p^{M^*} \tag{OA13}$$

$$\frac{\theta^S}{\theta^I}\frac{x^I}{x^S} = p^S \tag{OA14}$$

Household $i's$ optimal choice of location k^* is given by:

$$k^* = \begin{cases} u & \text{if} \quad \frac{\widetilde{c}^{*1-\sigma}}{1-\sigma} - \chi_1(AOD^u)^{\chi_2} > \frac{\widetilde{x}^{*1-\sigma}}{1-\sigma} - \chi_1(AOD^a)^{\chi_2} + \epsilon_i \\ a & \text{otherwise} \end{cases}$$

Letting $F(\epsilon)$ denote the cumulative distribution function of idiosyncratic amenity values ϵ, and with the marginal household's value ϵ^* defined by (17), the aggregate share of the population living in the urban area must thus satisfy:

$$\frac{L^{I,u}+L^S}{\bar{L}} = F(\frac{\widetilde{c}^{*1-\sigma}}{1-\sigma} - \chi_1(AOD^u)^{\chi_2} - \frac{\widetilde{x}^{*1-\sigma}}{1-\sigma} + \chi_1(AOD^a)^{\chi_2}) \tag{OA15}$$

Aggregate Conditions: Finally, competitive equilibrium requires that the domestic market for services clears (25), the government's budget constraint is satisfied (18), the national budget constraint holds (26), and that the country's labor market (24) clears.

OA3. Additional Model Results

Table OA3 shows a version of the sensitivity analysis assuming that policy revenues are rebated lump-sum to households.

Table OA3: Counterfactual results for South Africa in base year 2010 with lump-sum rebates.

Panel A: Overall Impacts								
	Agg. Exposure (AOD×bil.)	Agg. Exposure %Δ	Urban Pop. Share	Urban Exposure %Δ	Rural Exposure %Δ	Agg. Welfare %Δ		
Baseline	0.00424	-	0.62	-	-	-		
Oil Tax	0.00412	-2.77	0.60	-7.69	6.15	-0.011		
Burning Tax	0.00421	-0.59	0.62	-1.43	0.92	-0.002		
Coal Tax	0.00361	-14.92	0.57	-31.45	15.00	-0.047		
Panel B: Rural Impacts								
	Industry Output ($bil.)	Industry Empl. (bil.)	Ag. Output ($bil.)	Ag. Empl. (bil.)	Ag. Burning (MT)	Coal Use (ktoe)	Oil Use (ktoe)	AOD
Baseline	53.2	0.015	1471.5	0.004	5.3	24.1	1.6	0.083
Oil Tax	57.7	0.016	1406.3	0.003	5.1	26.0	1.4	0.083
Burning Tax	55.7	0.015	1276.5	0.003	4.5	24.7	1.5	0.083
Coal Tax	60.4	0.017	1590.8	0.004	5.7	23.2	1.9	0.083
Panel C: Urban Impacts								
Policy	Industry Output ($bil.)	Industry Empl. (bil.)	Services Output (units)	Services Empl. (bil.)		Coal Use (ktoe)	Oil Use (ktoe)	AOD
Baseline	122.9	0.007	2158.2	0.023		82.6	17.6	0.091
Oil Tax	113.1	0.007	2104.4	0.022		79.8	14.8	0.087
Burning Tax	121.3	0.007	2150.2	0.022		81.8	17.5	0.090
Coal Tax	95.6	0.006	2019.0	0.021		57.8	17.2	0.069

Note: *Each panel reports outcomes in four cases, baseline, with an oil tax, a tax on agricultural burning, and a coal tax. The top panel reports country level statistics. The middle panel reports outcomes for rural areas, and the bottom panel reports on the urban area. Exposure is measured in AOD times population in billions.*

Figure OA3 shows a version of the sensitivity analysis assuming that policy revenues are rebated lump-sum to households.

Figure OA3: Sensitivity Analysis: Level Change in Exposure per 1% Change in Parameter

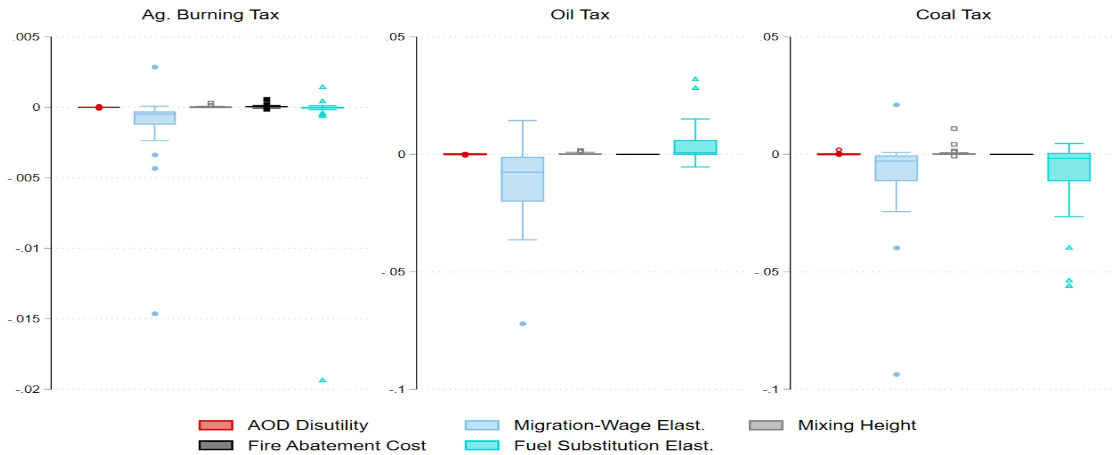

Note: *Sensitivity of results to five key parameters: AOD disutility, the migration-wage elasticity, atmospheric mixing height, agricultural burning abatement costs, and the elasticity of substitution across energy inputs. For each triplet of parameter $\times$ policy experiment $\times$ country, we compare the predicted effects of the policy on aggregate particulate exposure in the benchmark (with rebates) to an alternative calibration where the parameter in question is increased by +1%. The figure describes the results of these experiments with box plots of the distribution of the percentage point difference in predicted exposure effects. The box spans the 25th-75th percentile, the line represents the median, and the whiskers represent 1.5 times the inter-quartile range.*

OA4. Calculating cross-border particulate flows

Figure OA4 illustrates the boundary between two hypothetical regions where AOD is constant within each region. The arrows illustrate wind velocity across the border. For the sake of illustration, each instance of V_{BA} has velocity 2 and reflects the East-West wind velocity across the AB boundary. Letting the length of the solid bar at lower center be one unit distance, wind V_{BA} operates across two units of length. Therefore, the East-West transport of particulates is given by the length of the border over which wind travels from B into A, times the velocity of the wind, times mixing height, times the concentration of particulates in region B. Let λ denote mixing height and recall that ρ converts AOD to concentration, transport from region B to A is given by,

$$2 \times \lambda \times V_{BA} \times \rho \times \text{AOD}_B$$

Performing a similar calculation for flows from A to B and summing, we have net flows from A to B

$$F_{BA} = (2 \times \lambda \times V_{BA} \times \rho \times \text{AOD}_B) - (3 \times \lambda \times V_{AB} \times \rho \times \text{AOD}_A)$$

Figure OA4: Calculation of cross-boundary flows

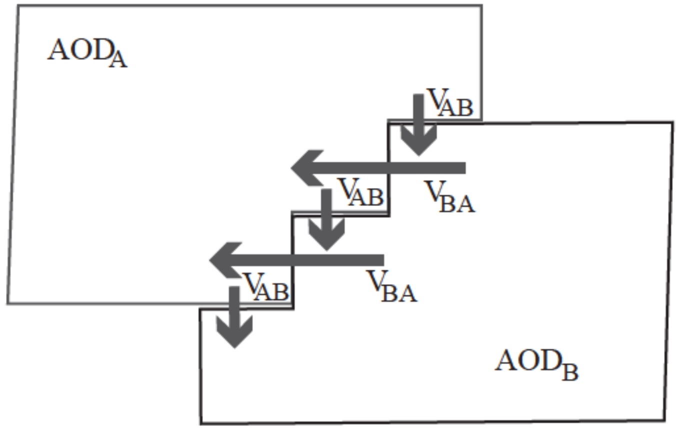

Note: *Logic for calculating the mass of cross-border particulate flows from gridded AOD and wind data.*

This is exactly the way that we calculate flows in practice, with one exception. Where we have here assumed that there is no pixel level variation in AOD within a region, in practice, the wind operates on whatever AOD we measure in its own pixel.

Our model will ultimately require two further structural parameters to describe flows across-borders. The first is border length. This is trivial to compute, and in this case, the border between regions A and B is 5 units long. The second parameter is the velocity of the cross-border wind, $v_{BA}\,(= -v_{AB})$. This is a complicated quantity because, to summarize cross-border wind, we must describe the direction it travels and the length of the border over which it operates. For the purpose of the model, wind velocity is defined as the velocity that explains the actual observed transfer of particulate mass across the border. That is, $v_{AB}\rho\lambda\text{AOD}_A \equiv F_{AB}$.